# Analysis of angiogenic and antiangiogenic drugs in turquoise killifish and zebrafish wound healing models

Master's Thesis

University of Turku

MSc Degree Programme in Biomedical Sciences

Drug Discovery and Development

September 2021

Johanna Örling

Supervisor: PhD Ilkka Paatero

Turku Bioscience Center, University of Turku

Institute of Biomedicine

Abstract

UNIVERSITY OF TURKU
Institute of Biomedicine, Faculty of Medicine

ÖRLING, JOHANNA: Analysis of angiogenic and antiangiogenic drugs in turquoise killifish and zebrafish wound healing models
Master's Thesis, 75 p, 3 appendices
MSc Degree Programme in Biomedical Sciences/Drug Discovery and Development
September 2021

---

Impaired wound healing is an ever-increasing worldwide burden to human health affecting especially aged population. Wound healing is a complex process in which angiogenesis has a significant role. Recent data suggest that compounds having angiogenic effects could improve wound healing. The aim of this study was to investigate the effects of different angiogenic (roxadustat, tazarotene, deferoxamine, sodium nitroprusside and cobalt chloride) and antiangiogenic (semaxanib) compounds in zebrafish and turquoise killifish wound healing models. In addition, the purpose was to study the effects of aging on wound healing by comparing the regeneration of caudal fin between young and old fish.

The results of the study showed that the regeneration of caudal fin in old zebrafish was significantly impaired when compared to young zebrafish. The inhibitory effect of semaxanib on fin regeneration was observed in both larval zebrafish and old turquoise killifish wound healing models. In turquoise killifish, this finding was also confirmed by qRT-PCR as lowered expression of *cd34* and by histology as reduced amount of collagen in the regenerated caudal fin. However, the regeneration of caudal fin in larval zebrafish and old turquoise killifish was not improved after the treatment with angiogenic compounds.

In conclusion, both aged zebrafish and aged turquoise killifish can be used to model wound healing during aging. However, no improvement on wound healing was observed with angiogenic compounds. Further investigation is needed in order to validate the fish wound healing models and to find novel treatments for wound healing.

Key words: wound healing, angiogenesis, zebrafish, turquoise killifish

# Table of Contents

# 1. Introduction

## 1.1 The challenge of impaired wound healing

Impaired wound healing is an ever-increasing worldwide burden to human health. In Europe alone, 1.5-2 million people suffer from wounds, either acute or chronic. (Lindholm and Searle, 2016) It has been estimated that in developed countries the treatment expenses caused by chronic wounds cover 3-5.5% of the total healthcare costs (Posnett & Frank, 2008; Philips et al., 2016). Poor wound healing can be associated to aging or several underlying diseases, for instance diabetes, vascular disease and cancer, or other conditions, such as injury, local-pressure effects or infection (Eming et al., 2014). Problems associated with wounds are not only physical, but also mental and social having a great impact on the quality of life in patients (Lindholm and Searle, 2016). Impaired wound healing may eventually become a mortal condition for the patient (Eming et al., 2014). For instance, 5-year mortality rate associated to amputations caused by diabetic ulcers is 50% (Sargen et al., 2013).

The treatment for chronic wounds is limited due to the complex mechanisms behind impaired wound healing. As the prevalence of many chronic diseases associated with poor wound healing is increasing, the need for deeper understanding of wound healing and new therapies is evident. One of the challenges related to the development of new treatments is the lack of preclinical animal models. The complex molecular mechanisms involved in human wound healing makes it difficult to develop models that would properly mimic human condition. Also, clinical research is challenging due to complex and variable patient population with comorbidities. (Eming et al., 2014)

## 1.2 The phases of wound healing

### 1.2.1 Hemostasis

Wound healing in human is a complex process consisting of four overlapping phases (figure 1) and involving several different cell types both locally and systemically (Rajendran et al., 2018). The first phase of wound healing called hemostasis starts immediately after injury and can last up to several hours (Reinke and Sorg, 2012). Acute

hypoxia in wound generates reactive oxygen species (ROS), which in turn causes vasoconstriction and reduces blood flow that are important for the protection of initial wound and thrombus formation (Dunnill et al., 2017). When the blood components expose to the subendothelial layer of the blood vessel wall, hemostasis is initiated with the help of vasoconstriction and platelet aggregation forms the first hemostatic plug. This leads to the initiation of clotting cascade. The formation of thrombin from prothrombin results in the generation of fibrin, which forms the blood clot with platelets and fibronectin. (Thiruvoth et al., 2015) Blood clot also has a defensive role against microbes, and it serves as a matrix for the inflammatory cells. The degranulation of platelets leads to the release of chemoattractants, vasoconstrictors and activation factors. (Sen and Roy, 2012)

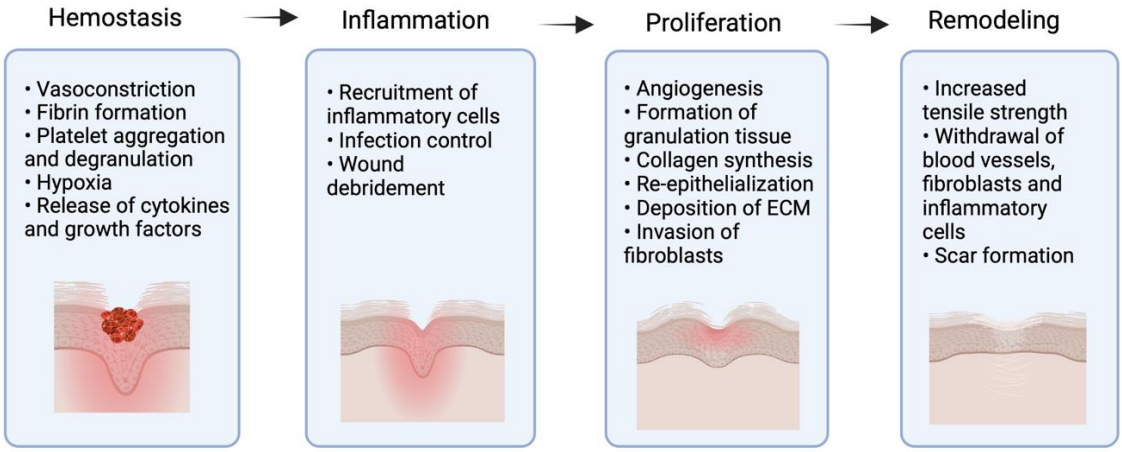


**Figure 1.** The phases of wound healing. Normal wound healing proceeds via four overlapping phases. Created with BioRender.com.

### 1.2.2 Inflammation

Hemostasis is followed by the inflammatory phase in wound healing. This phase typically lasts from 1 to 3 days. (Reinke and Sorg, 2012) Inflammatory response activates both systemic and local defense reactions leading to the recruitment of neutrophils, macrophages and lymphocytes. The first white blood cells to populate the wound are neutrophils that harness several different strategies to decontaminate the wound. (Roberts and Tabares, 1995) Neutrophils secrete antimicrobial peptides and proteases and generate ROS (Nathan, 2006). Monocytes take their place after neutrophils as predominant inflammatory cells in the wound and differentiate into macrophages (Thiruvoth et al., 2015). Macrophages phagocytize apoptotic neutrophils, which then results in the

elimination of chemokines from the wound area, hence inhibiting further leukocyte invasion (Martins-Green et al., 2013). Macrophages have a crucial role in wound closure (Eming et al., 2007), and several growth factors and cytokines are also produced by them (Novak & Koh, 2013). Growth factors such as FGF, VEGF (also known as VEGF-A), TGF-β, TGF-α and PDGF are involved in attracting and activating fibroblasts, keratinocytes and endothelial cells. These factors also induce cell proliferation, synthesis of ECM and have a role in angiogenesis. (Eming et al., 2007; Miao et al., 2013) Finally, lymphocytes appear at the wound site and exert a specific reaction to foreign material and microbes (Martins-Green et al., 2013).

### 1.2.3 Proliferation

The third phase of wound healing, called proliferative phase, is characterized by major events, such as re-epithelialization, angiogenesis, deposition of ECM and invasion of fibroblasts (Thiruvoth et al., 2015). It starts around 4 days post injury and can last up to 3 weeks (Reinke & Sorg, 2012). Fibroblasts become the predominant type of cells in proliferation phase and are activated by different growth factors (Thiruvoth et al., 2015). They start to proliferate and produce hyaluronic acid, type III collagen, fibronectin, and proteoglycans in order to construct new ECM and a scaffold for the migration of keratinocytes (Singer and Clark, 1999).

Fibroblasts and macrophages secrete angiogenic factors, such as VEGF and angiopoietin 1 (Ang-1) (Johnson and Wilgus, 2014; Kazemi-Lomedasht et al., 2015). New blood vessels start to develop from preexisting vessels during the process of granulation tissue formation. Granulation tissue gradually replaces fibrin matrix and consists of blood vessels, fibroblasts and macrophages embedded in the matrix of collagen, fibronectin and hyaluronic acid. (Thiruvoth et al., 2015)

Re-epithelialization starts in the early phase of wound healing. Keratinocytes at the wound edges are activated by EGF and TGF-β released by the platelets and start to proliferate and migrate in order to cover the wound. (Werner et al., 2007; Gillitzer and Goebeler, 2001) Matrix metalloproteinases (MMPs) help keratinocytes in their migration through the matrix and further promote re-epithelialization (Stevens and Page-McCaw, 2012).

### 1.2.4 Remodeling

The final phase of wound healing called remodeling starts approximately 3 weeks after injury lasting up to one year or even longer (Reinke and Sorg, 2012). Hypoxia in wound bed subsides when the re-epithelialization of the wound progresses. These changes in hypoxic conditions may contribute to vessel pruning that takes place during the remodeling. (Rodriguez et al., 2019) The tensile strength in the tissue improves by degradation, reorganization and resynthesis of ECM (Gonzales et al., 2016). The surface of the wound is covered by keratinocytes and the recreation of new stratified epidermis progresses from the wound borders towards the inner part of the wound (Martin, 1997). As the wound closes, the degradation of type III collagen leads to the increased synthesis of type I collagen. Several growth factors, such as TGF-β1 and FGF are involved in the regulation of collagen synthesis. (Gonzales et al., 2016) The thickening of collagen fibers and their parallel rearrangement increases the tensile strength of the tissue (Doillon et al., 1985). Due to apoptosis, emigration and other unknown cellular mechanisms, inflammatory cells, fibroblasts and majority of the blood vessels start to withdraw from the wound leading to scar formation, which is the final outcome in wound healing (Gonzales et al., 2016).

## 1.3 Angiogenesis and wound healing

### 1.3.1 The phases of angiogenesis

Angiogenesis is a complex, but an essential process in normal wound healing. It is typically observed during tissue repair, but also in several disease states. (Johnson and Wilgus, 2014) Proliferation, migration and differentiation of endothelial cells into newly formed vasculature is needed during the sprouting of new vessels (Carmeliet and Jain, 2011). Nutrients and oxygen are transported via capillaries into tissues and waste products are removed through them (Honnegowda et al., 2015). The process of angiogenesis can be divided to three distinctive phases: quiescence, activation and resolution. In healthy tissue, blood vessels stay at the quiescent state. The inner surface of the quiescent vessel is lined with endothelial cells called phalanx cells. The barrier between these cells is created by tight cell-cell adhesion and assists in maintaining blood flow. The cell-cell contacts of the quiescent endothelial cells begin to loosen prior to activation by

angiogenic factors. When the pericytes detach from the outer surface of the vessel and the basement membrane is degraded by MMPs, routes for the development of new sprouting vessels are formed. (Carmeliet and Jain, 2011) Growth of the new sprout is orchestrated by a single endothelial cell called tip cell. Tip cells conduct the vascular outgrowth by responding to the gradient of angiogenic factors. (Gerhardt et al., 2003) Adjacent endothelial cells start to proliferate and migrate towards the tip cell leading to the elongation of the newly formed vessel. Finally, in the resolution phase of angiogenesis the sprouts will fuse with nearby sprouts for establishing blood flow. By contrast, unperfused nonfunctional sprouts will regress. (Carmeliet and Jain, 2011)

### 1.3.2 Angiogenesis in wound healing

Angiogenesis during wound healing is initiated immediately after injury (Honnegowda et al., 2015). Several angiogenic factors, such as VEGF, PDGF and Ang-1, are released by platelets, macrophages and monocytes for stimulating the proliferation, migration and tube formation of endothelial cells (Hellberg et al., 2010; Li et al., 2001). The exposed endothelial cells release MMP-2 in order to promote the dissolution of the basement membrane, which is a crucial step for angiogenesis (Nguyen et al., 2001). Proteases breaking down the tissue matrix also release angiogenic stimulators (Bootle-Wilbraham et al., 2001). Hypoxia plays a major role in wound angiogenesis. During the vascular proliferation, expression of hypoxia-inducible factor 1α (HIF-1α) triggers the production VEGF (Acker and Plate, 2003). Nitric oxide (NO) released by endothelial cells in response to hypoxia promotes both angiogenesis and vasodilatation (Smith et al., 2009). The stabilization of the vasculature is orchestrated by Ang-1, tyrosine kinase with immunoglobulin -like and EGF-like domains 2, pericytes and smooth muscle cells (Carmeliet and Jain, 2011). At the final stages of wound healing angiogenesis is suppressed (Kumar et al., 2009). As hypoxia and inflammation in the tissue subside, the increased levels of growth factors become normalized (Honnegowda et al., 2015).

### 1.3.3 Angiogenic switch

It is believed that the process of angiogenesis is controlled by the changing levels of angiogenic and antiangiogenic factors in the surrounding microenvironment of the vasculature. Angiogenic mediators, such as VEGF, PDGF and TGF-β, are involved in

stimulating angiogenesis whereas antiangiogenic mediators, such as angiostatin and endostatin, inhibit angiogenesis. (Honnegowda et al., 2015) Blood vessels stay at the quiescent state when the signal level from antiangiogenic mediators exceeds the level of angiogenic factors. When there is a shift in the balance between these opposite factors, endothelial cells sense the shift and prepare for angiogenesis. This phenomenon is called the angiogenic switch (figure 2) originally used for describing the regulation of angiogenesis in tumor growth. (Hanahan and Folkman, 1996)

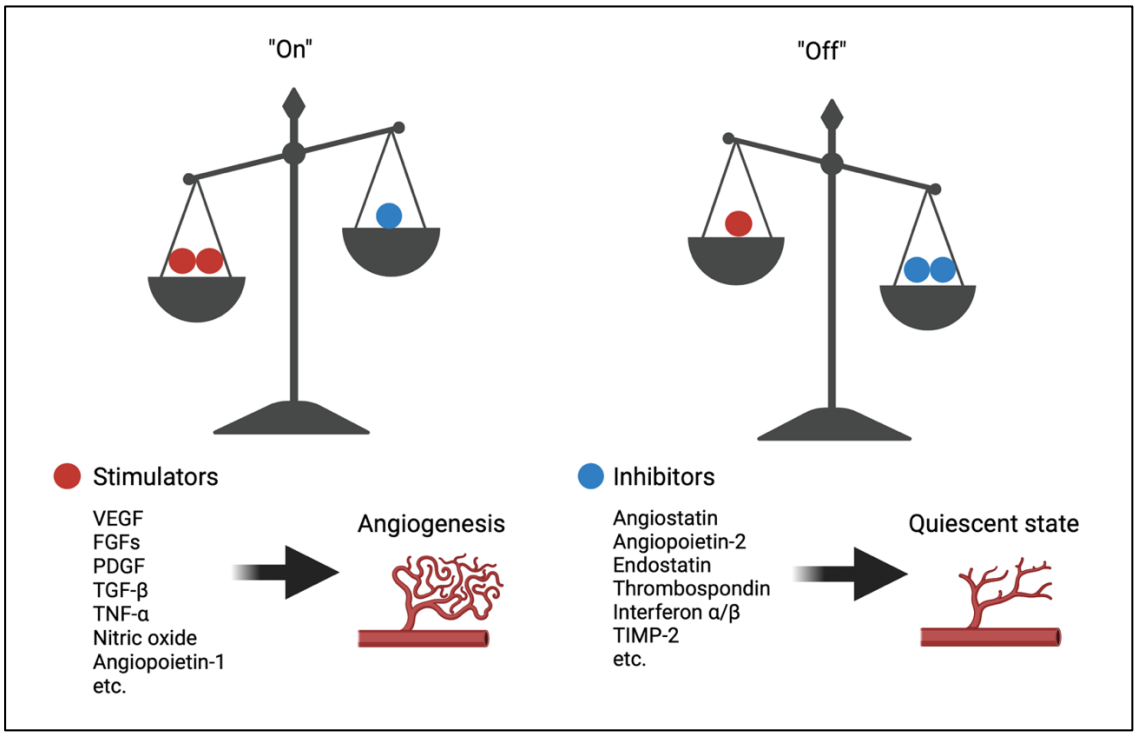


**Figure 2**. Angiogenic switch. When the switch is "on", angiogenesis is triggered by several different stimulators. When the switch is "off", inhibitory mediators are involved in maintaining blood vessels at the quiescent state. Angiogenic signal can be released for instance by inflammatory, hypoxic or tumor cells. Created with BioRender.com.

## 1.4 Complications in wound repair

### 1.4.1 Aging-related changes affecting wound repair

Fetal skin has an amazing capability for scarless tissue regeneration (Rowlatt, 1979). This capacity in fetus is conserved across several mammalian species (Adzick and Longaker, 1992). Also, the rate of healing is faster in fetal wound healing and results in complete restoration of all skin layers (Rodriquez et al., 2019). However, the transition to scar formation from scarless wound healing begins already from the third trimester (Occleston

et al., 2008). During aging, the physiological changes start to complicate wound healing even more. Advanced age of over 60 is considered an independent risk factor for impaired wound healing. (Sgonc and Gruber, 2013) Aging-related changes affect all phases of wound healing. For instance, during hemostasis platelet aggregation and degranulation are typically increased. (Ashcroft et al., 2002) Delayed infiltration of leucocytes characterize the inflammation process (Ashcroft et al., 1998). Due to impaired macrophage function, the secretion of proinflammatory mediators is increased and the production of VEGF is decreased (Ashcroft et al., 2002). Recent findings suggest that insufficiency in VEGF signaling could actually be one the primary drivers in overall aging process (Grunewald et al., 2021).

In proliferation phase, delays in the deposition of ECM and collagen together with impaired angiogenesis and re-epithelialization are typical age-related changes (Ashcroft et al., 2002). Impaired collagen deposition is due to the reduced sensitivity to TGF-β1 (Mogford et al., 2002) in addition to the decreased fibroblast proliferation and migration (Xia et al., 2001). Impaired keratinocyte proliferation and migration further contributes to the delayed re-epithelialization in the wound area (Xia et al., 2001). Reduced HIF-1α signaling as an indicator of decreased response to hypoxia is involved in the delayed angiogenesis in elderly (Chang et al., 2007). In aged skin, the delay in microvascular response leads to impaired thermoregulation and hypoperfusion in tissue, which in turn inhibits the angiogenic phase of wound healing to initiate. Aging-related decrease in vascular density and increase in disorganization of blood vessels further contribute to the impairment of transport capacity in skin vasculature. (Bentov and Reed, 2014) Increased scarring and decreased collagen turnover characterize the remodeling phase during aging (Sgonc and Gruber, 2013).

Many factors are known to affect wound healing during aging. For instance, reduced levels of estrogen and androgen complicate wound healing by impairing ECM deposition and inflammation control (Sgonc and Gruber, 2013). Malnutrition is fairly common in elderly, and together with impaired mobility it can lead to chronic pressure ulcers (Mathus-Vliegen, 2004). With advanced age, comorbidities with medications that impair wound healing also become more common. Systemic glucocorticoids delay wound healing by inhibiting the inflammatory phase whereas chemotherapeutic drugs impair for instance cell proliferation, angiogenesis and ECM formation. Also, many diseases that

are common in elderly people, such as diabetes or peripheral arterial disease, contribute to complications in wound healing. (Sgonc and Gruber, 2013)

### 1.4.2 Chronic wounds

The mechanisms underlying behind impaired wound repair are poorly understood, but several factors are known to complicate wound healing, such as infection in the wound, trauma or ischemia. Complications in any of the wound healing phases lead to chronic wounds. (Frykberg and Banks, 2015) Wound is considered chronic if it does not heal in 12 weeks. The primary risk factors for chronic wounds are aging and diabetes. (Wilkinson and Hardman, 2020) Typically, chronic wounds are stuck in the inflammatory phase. They share many similarities despite different underlying etiologies, such as high levels of ROS, proteases, senescent cells with impaired capacity to proliferate and increased levels of proinflammatory cytokines as well as dysfunctional stem cells. (Frykberg and Banks, 2015) Ongoing tissue injury stimulates the influx of immune cells leading to the amplified cascade of proinflammatory cytokines, which in turn leads to the elevated protease levels (McCarty and Percival, 2013). High levels of ROS produced by immune cells damage proteins in ECM leading to the stimulation of inflammatory cytokines and proteases (Schreml et al., 2010). Elevated levels of proteases result in the proteolytic destruction of synthetized ECM. More inflammatory cells are attracted by growth factors, which in turn amplifies the inflammation. (McCarty and Percival, 2013) Cellular senescence is typically observed in several cell types, such as in keratinocytes, fibroblasts, macrophages and endothelial cells (Frykberg and Banks, 2015). Senescent cells may also become hypersecretory and produce high amounts of proteases and pro-inflammatory cytokines (Childs et al., 2015). In addition, microbiota is known to play a significant role in chronic wounds, such as in diabetic foot ulcers (Kalan et al., 2019).

## 1.5 Current treatment of chronic wounds

Correct wound treatment requires a holistic approach in which the underlying causes are investigated, and the appropriate treatment is selected based on the patient's overall disease status. For instance, in the management of diabetic ulcers, the treatment starts with careful control of blood glucose levels. Depending on the underlying causes, other

methods utilized in the treatment of ulcers are compression, exercise, pressure distribution, offloading and nutritional support, for instance. (Bowers and Franco, 2020)

Local wound care also consists of several treatments. Debridement of the necrotic tissue from the wound has been shown to result in 70.8% rate in wound healing (Wilcox et al., 2013). Also, the removal of biofilm from the wound with antimicrobial washes is essential (Bowers & Franco, 2020). The invisible multicellular community called biofilm is associated in 80% of wound infections (Davies, 2003) and can stall the healing process in the inflammation phase (Lebrun and Kirsner, 2013). Depending on the etiology of the wound, appropriate antiseptic or antibiotic treatment should be started. In the case of systemic infections, oral antibiotics should be introduced. (Bowers and Franco, 2020) Chronic wounds should also be kept moist with proper dressings as moisture prevents infections and accelerates the healing (Field and Kerstein, 1994).

During recent years, the search for new treatments for wound healing has been fierce. 3D printing has enabled complex material development, and for instance in 3D wound dressings several types of materials can be combined with different drugs. 3D printed biomaterials mimic the extracellular matrix, and in the future, it could even be possible to produce skin with 3D printers (Okur et al., 2020). Growth factors have also been studied for years for their potential in wound healing, but the results have been modest so far. The first and only growth factor therapy, PDGF, approved by the Food and Drug Administration is used for the topical treatment of diabetic ulcers (Kiwanuka et al., 2012). Stem cell and RNA therapies have also shown considerable potential in wound healing but results from large clinical trials are still lacking (Okur et al., 2020).

## 1.6 Angiogenic and antiangiogenic compounds

Several compounds or registered drugs with different indications have been shown to have angiogenic properties. Some examples of these are roxadustat, deferoxamine and cobalt chloride, that act via HIF pathway (figure 3, table 1). For instance, inhibitor of HIF propyl hydroxylase, roxadustat, or FG-4592, is an oral small molecule and the first drug in a new class of HIF propyl hydroxylase inhibitors (AstraZeneca, 2021). It was first approved for the treatment of anemia of chronic kidney disease in China in 2018 (FibroGen, 2018). Inhibition of propyl hydroxylase reduces the breakdown of HIF-α and

promotes its transcriptional activity. Increased endogenous production of erythropoietin via activation of HIF pathway promotes erythropoiesis and improves iron absorption. (Besarab et al., 2015) Deferoxamine, also known as desferal or desferrioxamine, is a small molecule used for treatment of iron or aluminum toxicity. As a chelating agent it binds to free aluminum or iron in the bloodstream forming stable complexes that are eliminated via kidneys. (National Center for Biotechnology Information, 2021a) Cobalt chloride ($CoCl_2$) is an inorganic compound that inhibits the activity of asparaginyl and prolyl hydroxylase and proteasome degradation of HIF-1α (Jaakkola et al., 2001) in addition for preventing the incorporation of iron to produce heme (Maines & Sinclair, 1977), which then results in chemical hypoxia.

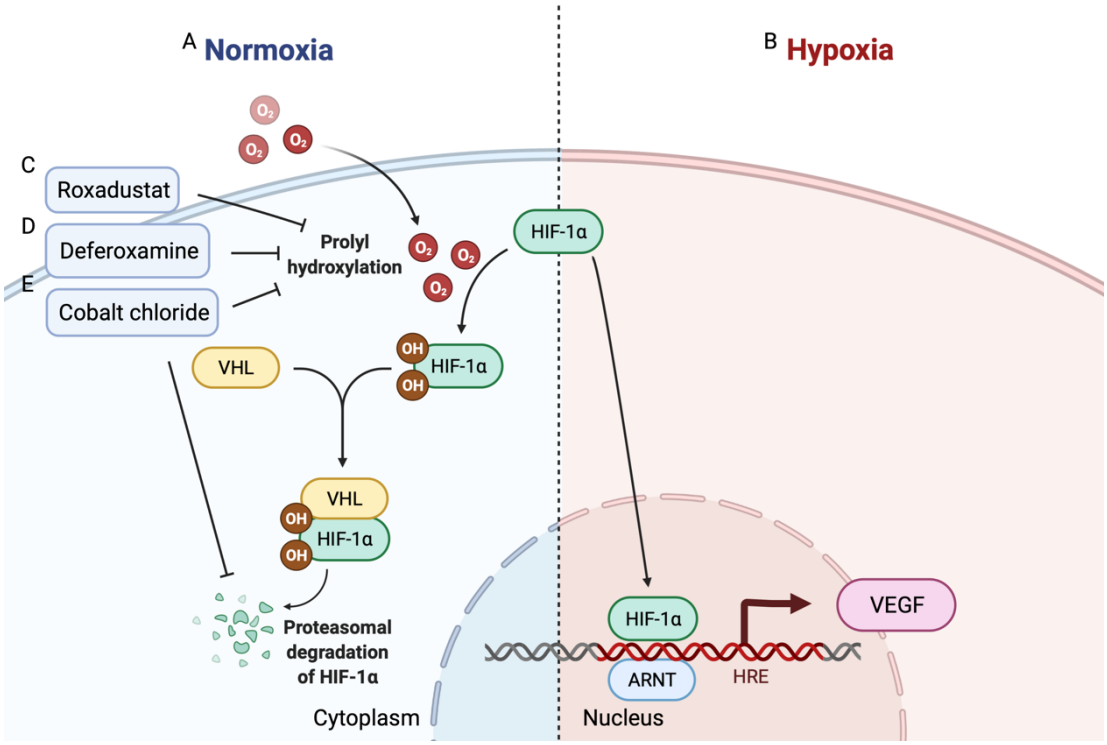


**Figure 3**. A simplified figure of the HIF pathway and the mechanisms of action of roxadustat, cobalt chloride and deferoxamine. A) Under normoxia HIF-1α breaks down by proteasomal degradation. The degradation process is regulated by oxygen when hydroxyl groups are added to HIF-1α. After this, von Hippel-Lindau (VHL) protein is able to form a complex with HIF-1α, which eventually leads to its degradation. B) During hypoxia, the degradation of HIF-1α is protected and it cumulates in nucleus. In nucleus, HIF-1α associates with transcription factor aryl hydrocarbon receptor nuclear translocator (ARNT) and binds to a specific DNA sequence called hypoxia response element (HRE), in the genes regulated by hypoxia. This further leads to the upregulation VEGF, for instance. Roxadustat (C), deferoxamine (D) and cobalt chloride (E) all inhibit propyl hydroxylase, which is involved in the degradation of HIF-1α. In addition, cobalt chloride inhibits the proteasomal degradation of HIF-1α. Adapted and modified from "HIF Signaling", by BioRender.com (2021). Retrieved from https://app.biorender.com/biorender-templates.

Also, other drugs with different mechanisms of actions, such as sodium nitroprusside and tazarotene have been shown to improve angiogenesis (table 1). Vasodilator sodium nitroprusside is a drug used for the treatment of acute hypertension and related conditions. As a prodrug, it reacts with the sulfhydryl groups on erythrocytes and produces NO that relaxes vascular smooth muscles leading to peripheral vasodilation both in veins and arteries. (Holme and Sharman, 2020) NO is also involved in several other physiological processes, such as in cell proliferation, apoptosis and differentiation (Alderton et al., 2001), and it is also an important modulator of angiogenesis via VEGF (Conway et al., 2001).

Tazarotene is a third-generation retinoid used topically for the treatment of acne, plaque psoriasis and photodamaged skin. The exact mechanism of action of this small molecule is unclear, but it is an agonist for all the retinoid acid receptor subtypes RARa, RARb and RARg, and is possibly also involved in gene expression modifications (National Center for Biotechnology Information, 2021b). Retinoid acid signaling has been shown to have a significant role in the regeneration of zebrafish fin, especially in the formation blastema (Blum and Begemann, 2012).

Antiangiogenic drugs are widely used in the treatment of different cancers to inhibit tumor growth by suppressing the vascularization in tumors. Small molecule semaxanib, or SU5416, is a selective tyrosine-kinase inhibitor of vascular endothelial growth factor receptor 2 (VEGFR-2/Flk-1/KDR, table 1). It reached phase III clinical trials in 2002 for the treatment of advanced colorectal cancer, but due to discouraging results, the trial was terminated prematurely (Cancer Network, 2003). Despite of the discontinued development of semaxanib, it is still being widely used for investigative purposes, particularly in the studies concerning receptor tyrosine kinases.

**Table 1.** Angiogenic (A) and antiangiogenic (AA) compounds selected for the study with mechanisms of actions, relevant findings from previous studies and references.

| **Compound** | **Mechanism of action** | **Findings from earlier studies** | **References** |
|---|---|---|---|
| Cobalt chloride (A) | Inhibition of HIF propyl hydroxylase and proteasome degradation | Increased angiogenesis in the wounds of diabetic mice*<br><br>Enhanced caudal fin regeneration in zebrafish† | *Mace and Paydar, 2007<br><br>† Sagayaraj and Malathi, 2017 |
| Deferoxamine (A) | Inhibition of HIF propyl hydroxylase | Accelerated wound healing in diabetic mice*<br><br>Improved wound healing in aged mice†<br><br>Angiogenic properties in wound healing, ischemia and bone regeneration‡ | *Hou et al., 2013<br><br>†Bonham et al., 2018<br><br>‡Holden and Nair, 2019 |
| Roxadustat (A) | Inhibition of HIF propyl hydroxylase | Increased angiogenesis and wound healing in diabetic rats*<br><br>Improved *in vitro* motility and proliferation of epidermal stem cells† | *Zhu et al., 2019<br><br>†Tang et al., 2018 |
| Sodium nitroprusside (A) | Formation of NO | Accelerates the formation of blood vessels in the trunk of larval zebrafish*<br><br>Angiogenic effects in rabbit cornea† | *Pelster et al., 2005<br><br>†Ziche et al., 1994 |
| Tazarotene (A) | Retinoid acid receptor activation<br><br>(Activation of VEGFR/VEGFR-Notch1/DLL4?†) | Promotion of endothelial tube branching and remodeling *in vitro,* enhanced growth of microvessels, accelerated wound healing *in vivo**<br><br>Improved wound repair in mice while administered in nanoparticle carriers† | *Al Haj Zen et al., 2016<br><br>†Liu et al., 2020 |
| Semaxanib (AA) | Inhibitor of VEGFR-2<br><br>(Inhibition of TGF-β†) | Antiangiogenic effects in cancer studies both *in vitro* and *in vivo**<br><br>Delayed wound healing in rats† | *Fong et al., 1999, Mendel et al., 2000<br><br>†Haroon et al., 2002 |

## 1.7 Fish as a model for wound healing

### 1.7.1 Regenerative capacity in fish

Tissue regeneration is a fascinating mystery among different organisms. Nonmammalian vertebrates, such as fish, have an astonishing capability for organ and tissue regeneration whereas in humans tissue regeneration is only limited. Cells form the foundation for regeneration, and the abundancy of cellular sources is one of the key factors determining the regenerative capacity. (Zhao et al., 2016) The cellular mechanisms for regeneration include the activation of progenitor or stem cells, dedifferentiation of cells to their progenitors and transdifferentation of tissue cells into another type of tissue cells (Jopling et al., 2011). Regenerative species either have certain amounts of stem cells preserved or have a potential in adult cells for dedifferentiation or transdifferentation. In most adult mammals, these mechanisms are however missing, thus their regenerative capacity is largely limited. (Knopf et al., 2011)

Many teleost fish, such as zebrafish, are able to reconstruct their fin after amputation from blastema, which is a group of cells having regenerative capability and also the primary cue for regeneration (Knopf et al., 2011). The regenerative process in fin starts from wound healing and proceeds via blastema and fin ray formation to distal outgrowth and differentiation of certain, specialized structures. Amputated wound site in fish fin is covered with epithelium in 7 to 12 hours, and proliferation and thickening of the epidermal layer takes place in 24 hours. Differentiation occurs 48 hours post injury. In this phase, layers of basal cells in addition to connective tissue populated with white blood cells are observed. Apical cap, the most distal part of the wound, occurs only by cell migration similarly as in skin. After the apical cap has been formed by epithelial cells, the remaining epidermal cells start to proliferate and the formation of blastema begins within four days after amputation. (Santos-Ruiz et al., 2002) Lineage-restricted progenitor cells that populate the fin tissue migrate to the site of amputation to blastema, which involves both activation and dedifferentiation of stem cells (Zhao et al., 2016). For instance, osteoblasts in fin dedifferentiate temporarily, migrate to blastema and finally redifferentiate into osteoblasts again (Knopf et al., 2011). After blastema formation, outgrowth of the fin begins by five to seven days after amputation (Misof and Wagner, 1992). Bone deposition above ray stumps connects the stumps to the newly formed

hemirays (Santos-Ruiz et al., 2002). Muscle tissue regeneration starts approximately seven days after injury and completes in 10 to 15 days (Ramachandran and Thangavelu, 1969).

Several different factors contribute to regeneration. For instance, regeneration may be influenced by certain genes. In zebrafish the expression of growth factor *Fgf20a* suggests that regeneration genes are carried by both nonregenerative and regenerative species but are involved in regeneration only in the latter (Zhao et al., 2016). *Fgf20a* is expressed in zebrafish after amputation and has a role in the initiation of regeneration (Whitehead et al., 2005). In mammals, there is no association of orthologue of *Fgf20a* with regeneration (Zhao et al., 2016).

Epigenetic regulators have been shown to modulate regenerative processes (Cho et al., 2013; Gornikiewicz et al., 2013). Differences in DNA methylation have an effect on the expression of regeneration-associated genes (Zhao et al., 2016). Histone modifications are also involved in zebrafish fin regeneration. For instance, the knockdown of histone deacetylase HDAC1 impairs fin regeneration. (Pfefferli et al., 2014)

Based on several studies it seems that the relationship between the regenerative capacity and advanced immune system in different animal species is inverse (Mescher and Neff, 2005; Aurora and Olson, 2014). For instance, in zebrafish, the capacity for regeneration in central nervous system is higher than in mammals and associates with weaker inflammatory response after injury than in mammals (Kyritsis et al., 2014).

### 1.7.2 Turquoise killifish

Turquoise killifish (*Nothobranchius furzeri*) is a short-lived annual fish that naturally lives in the savannah pools in eastern Africa - area of distinct rainy and dry seasons. The embryos of turquoise killifish are extremely tolerant to drought and thus able to survive throughout the dry season in dry mud in a dormant state called diapause. During diapause the development of the embryos is halted. Embryos start to hatch when the ponds fill up with water during rainy season. After this, they grow fast becoming sexually mature in only 3 weeks. (Blazek et al., 2013a) The fish die when the ponds desiccate limiting their maximal lifespan in nature to under 12 months (Cellerino et al., 2016).

The species of turquoise killifish can be divided to several different strains, of which GRZ (figure 4) has the shortest median lifespan (Valdesalici and Cellerino, 2003). This inbred strain was named after its natural habitat in Gona Re Zhou National Park in Zimbabwe and was collected for laboratory use in 1968 (Jubb, 1971). Terzibasi et al. (2008) have reported a median lifespan of 9 weeks in GRZ. Its short lifespan is associated with fast aging, which can be seen for instance in aging biomarkers and in the behavior of the fish (Terzibasi et al., 2008). In addition to GRZ, there are also longer-lived strains available for laboratory use. For instance, outbred MZCS222 was collected in 2011 from Mozambik (Cellerino et al., 2016). Its median lifespan of 34 weeks has been reported for instance by Kosonen (2020).

Based on recent studies, the regenerative capability in aged turquoise killifish is impaired. Wendler et al. (2015) noticed in their studies with turquoise killifish strain MZM-0703 that young, 8-week-old killifish could regrow their caudal fin to its original length in 4 weeks whereas very old, 54-week-old fish could rebuild only half of the fin, respectively. This difference between young and very old fish was statistically significant already at 3 days after amputation (Wendler et al. 2015). Reduced regenerative capacity associated to aging is a phenomenon typical for mammals (Platzer and Englert, 2016). In fact, the aging of turquoise killifish resembles mammalian aging in many ways. Killifish have been reported to show mitochondrial dysfunction (Hartmann et al., 2011), telomere shortening in skin and muscles (Hartmann et al., 2009) and cellular senescence (Genade et al., 2005). The short lifespan and fast aging process of turquoise killifish makes it an excellent, cost-effective tool for aging research (Platzer and Englert, 2016). Based on the finding that turquoise killifish loses its regenerative capacity during aging, this fish species is also a potential model for investigating the mechanisms associated with aging-related decline in wound healing.

**Figure 4.** Turquoise killifish strain GRZ. Adult male of yellow morph in the front and smaller, dull female in the back. Turquoise killifish can grow up to 7.5 cm long (Blažek et al., 2013a).

### 1.7.3 Zebrafish

Zebrafish (*Danio rerio*) is a 2-5 cm long teleost (figure 5) naturally living in the freshwaters of South Asia (Aleström et al., 2020). In captivity the mean lifespan of outbred zebrafish is 3.5 years, but even as high age as 5.5 years has been reported (AnAge, 2021). Zebrafish has reached wide popularity as a cost-effective model organism in biomedical research due to its small size, rapid development, high fecundity and the fact that it is easy to breed and maintain in captivity (Nasiadka and Clark, 2012). Zebrafish show similar senescence during aging than humans. Spinal curvature is probably the most easily observed sign of aging in zebrafish and is likely due to muscle abnormalities. (Gerhard et al., 2002). Lipofuscin accumulation in liver is also observed in aged zebrafish in addition to retinal atrophy (Kishi et al., 2008), gene level response to oxidative stress (Malek et al., 2004) and decline in reproductive capacity (Kishi et al., 2008).

Zebrafish is one the most widely used vertebrate models for regeneration studies (Bernhardt et al., 1996; Poss et al., 2002). The regenerative capacity in zebrafish seems to be almost unlimited (Marques et al., 2019). For instance, caudal fin in zebrafish regenerates completely even after several amputations (Azevedo et al., 2011; LeClair and Topczewiski, 2010). However, subtle changes in the regenerated organs, such as in the pigmentation or the position of branched bony rays in fin have been seen (Azevedo et al., 2012).

At least for the heart, age does not seem to restrict the regenerative capacity in zebrafish (Itou et al., 2012), but the function of the heart may still be impaired resulting in asynchronous contraction of the regenerated area with unaffected heart (Gonzalez-Rosa et al., 2014). Itou et al. (2012) reported no decline in aged, 26 - 36-month-old zebrafish in the capacity for caudal fin regeneration. Also, Shao et al. (2011) compared the regeneration of the caudal fin between 4-, 12-, 18- and 28-month-old zebrafish and observed no correlation with age at 48 hours after amputation. However, when the regeneration was followed up until 30 days post amputation (dpa), they noticed that in 18-month-old fish the regenerative capacity is impaired starting from 20 dpa when compared to 4- and 12-month-old fish. At 30 dpa, the length of the caudal fin was 90% of its original length in 18-months old fish and respectively 95-98% in 4- and 12-month-old fish. Thus, these results suggest that in aged fish the ability to regenerate caudal fin is slightly impaired.

Most of the studies concerning regeneration are performed in adult zebrafish but depending on the study and the model in question, also larvae can be used. Using injured larvae, compounds can be tested for their pro-regenerative or inhibitory effects on regeneration. (Marques et al., 2019)

**Figure 5.** Zebrafish was originally named after its horizontal stripes across the body.

## 1.8 Aims of the study

Fish wound healing model is a valuable tool to study the mechanisms behind wound healing, but also for investigating the potential of different drugs in improving wound healing. Angiogenic compounds have been shown to improve wound healing in several *in vivo* studies. Thus, one of the aims of the present study was to investigate the potential

of different angiogenic compounds to improve wound healing in larval zebrafish and adult turquoise killifish wound healing models. In order to validate the wound healing models, also antiangiogenic compound was included in the study as a potential control.

In addition, the purpose was to study the effects of aging on wound healing by comparing the caudal fin regeneration between young and old zebrafish and turquoise killifish. Based on earlier somewhat conflicting studies, it was hypothesized in the present study that in 40-month-old zebrafish the regeneration of caudal fin is impaired when compared to young, 4-month-old zebrafish. As aging has been shown to impair wound healing at least in old turquoise killifish, the aim was also to investigate if certain genes involved in wound healing are affected during the regeneration of caudal fin in young and middle-aged turquoise killifish. Additionally, in order to perform wound healing studies with a convenient, fast-aging fish species, one of the aims of the present study was to set up turquoise killifish strain GRZ in laboratory. Caudal fin imaging and length measurements in addition to gene expression analyses and histology were selected as investigative methods in the present study.

## 1.9 Summary

Impaired wound healing is a significant burden to human health. In normal conditions, wound healing proceeds via four overlapping phases. Complications in any of these phases may lead to chronic wounds. In elderly people, wound healing is compromised due to physiological changes and possible underlying diseases. Angiogenesis also has a significant role in wound healing, and it is triggered for instance by hypoxia and VEGF. During aging, impaired response to hypoxia contributes to the delay in angiogenesis in wound healing. Angiogenic compounds have shown potential in improving wound healing *in vivo*. Zebrafish and turquoise killifish can be used to model wound healing due to their capacity to regenerate different tissues, such as fins. In the present study, the effects of aging and chosen angiogenic and antiangiogenic compounds on the regeneration of turquoise killifish and zebrafish caudal fin were investigated.

# 2. Results

## 2.1 Survival analyses between turquoise killifish strains GRZ and MZCS222

In order to perform wound healing studies with aged turquoise killifish, setting up a short-lived turquoise killifish strain GRZ in the laboratory was tried. However, several challenges were faced due to this. Only 10 fish from 2 different populations successfully developed from fertilized eggs into adults and finally reached their natural death. However, survival data was collected from the 10 fish that successfully developed into adults, and this data was compared with the survival data of turquoise killifish strain MZCS222 (figure 6). Collecting survival data from the different strains of turquoise killifish is important in each laboratory raising this fish species due to variable living conditions in each laboratory. Living conditions, such as food (Terzibasi et al., 2009) and tank water (Valenzano et al., 2006) can markedly affect the lifespan of turquoise killifish. The survival data of MZCS222 was collected from 4 populations from previous studies and partly also during the present study. Possible deaths were recorded daily. The results from the survival analyses indicate that the median lifespan of 14 weeks in GRZ is significantly shorter ($p < 0.0001$) than the median lifespan of 33 weeks in MZCS222.

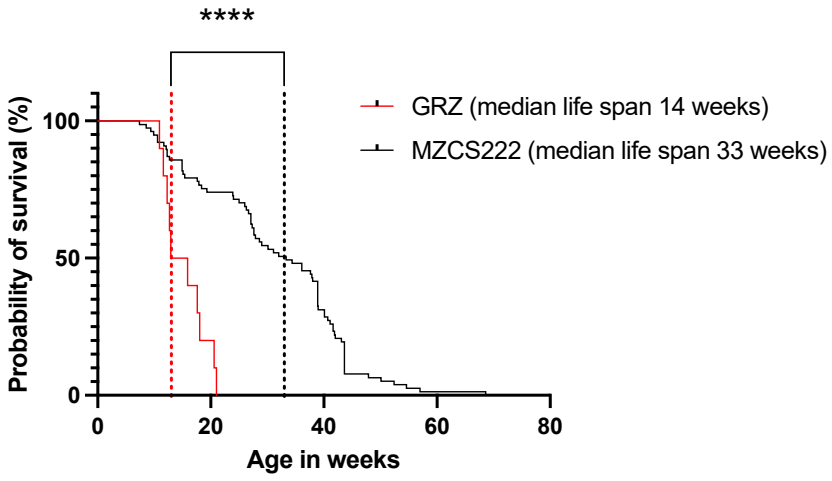


**Figure 6.** The survival rates of turquoise killifish strains GRZ and MZCS222. The survival analyses show that the median lifespan for GRZ is 14 weeks (red dashed line) and 33 weeks for MZCS222 (black dashed line). The difference between the median lifespan of these strains is statistically significant with the $p$ value of < 0.0001 (n=10 in GRZ and 77 in MZCS222). Statistical analysis was performed using Log-rank test. A $p$ value of < 0.05 was considered significant.

## 2.2 Wound healing studies with turquoise killifish strain MZCS222

### 2.2.1 Gene expression analyses from the drug study with old fish

The expression of chosen genes involved in angiogenesis was investigated from the regenerated pieces of caudal fins collected from a previous drug study with turquoise killifish strain MZCS222. In the study by Kosonen (2020), a piece of caudal was amputated from old (32 weeks) turquoise killifish, and the fish were treated with either angiogenic roxadustat or antiangiogenic semaxanib for 8 days. Control group received 0.01% DMSO. At the end of the study, a piece of the regenerated part of caudal fin was collected for gene expression analyses. To investigate the changes in angiogenesis in the regenerated caudal fin between the groups after 8-day drug treatment, the expression of angiogenesis-related genes vascular cell adhesion molecule 1 *(vcam1),* receptor tyrosine kinase with immunoglobulin-like and EGF-like domains 1 *(tie1),* cluster of differentiation-34 *(cd34)* and *vegfa* were analyzed in the present study. Housekeeping gene tata-box binding protein (*tbp)* was selected as a normalization gene. The results (figure 7) are presented as relative quantification values. Four replicates per sample were analyzed and sterile water was used as a negative control. The results from the gene expression analyses indicate no differences in most of the genes, but in *cd34* the difference between control and semaxanib group was statistically significant with the *p* value of 0.0103, and in *vegfa* the *p* value was close to significant being 0.0528.

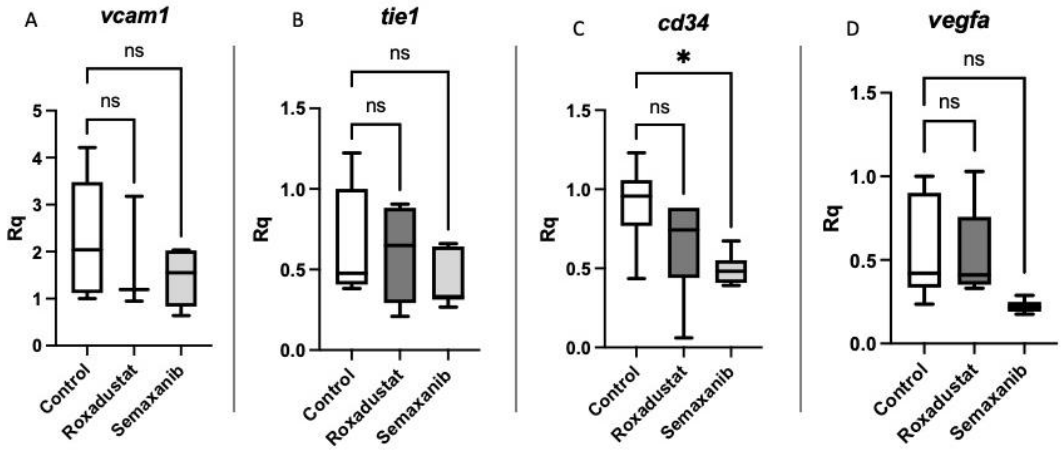


**Figure 7.** Expression of certain genes related to angiogenesis in the regenerated turquoise killifish strain MZCS222 caudal fin after 8-day treatment. No statistically significant differences were observed between the groups in (A) *vcam1*, (B) *tie1* or (D) *vegfa*. However, in (C) *cd34* there was a statistical difference between semaxanib and control group (**p* = 0.0103). n=6-7/group, but only 3 in roxadustat group for *vcam1*. The results were statistically analyzed using one-way ANOVA followed by Dunnett's multiple comparisons test. A *p* value of < 0.05 was considered significant.

### 2.2.2 Histological analyses from the drug study with old fish

The tissue level effects of roxadustat and semaxanib on the wound healing of turquoise killifish strain MZCS222 caudal fin were investigated by Masson-Goldner (MG) staining and phospho-histone H3 (PHH3) & collagen-binding adhesion protein 35 (CNA35) double staining. In the previous study by Kosonen (2020), half of the regenerated part of the caudal fin was stored in 10 % neutral buffered formalin after 8-day drug treatment. In the present study, those samples were embedded in paraffin in a frontal plane, sectioned and stained with MG for analyzing blood vessel density. Antibody for PHH3 and collagen probe CNA35 were used to calculate the mitotic cells and the amount of collagen in the tissue. The blood vessel analyses were performed in QuPath software for image analysis (Bankhead et al., 2017) whereas mitotic cells and collagen were analyzed in Fiji image analysis software (Schindelin et al., 2012). No statistically significant differences in blood vessel density were observed in roxadustat or in semaxanib groups when compared to control group (figure 8A). The amount of collagen was statistically lower ($p = 0.0387$) in semaxanib group when compared to control group after 8-day treatment (figure 9A). However, no significant effects of roxadustat on the amount of collagen in caudal fin were observed. In addition, no significant effects of roxadustat on mitotic cells in caudal fin were observed, but in semaxanib group the number of mitotic cells was statistically higher ($p = 0.005$) than in control group (figure 9B). Representative images as examples of the stainings are presented in figures 8B and 10.

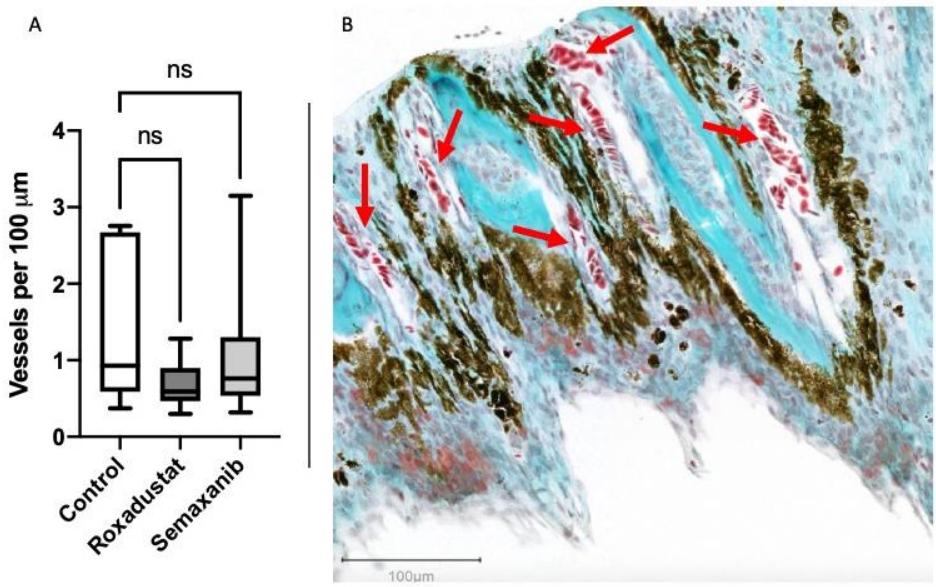


**Figure 8.** (A) Blood vessel density in the caudal fin of turquoise killifish strain MZCS222 after 8-day drug treatment. No statistically significant differences were observed in angiogenic roxadustat or antiangiogenic semaxanib groups when compared to control group (n=7/group). The results were statistically analyzed using one-way ANOVA. *p* value of ≤ 0.05 was considered significant. (B) An example of MG staining on turquoise killifish caudal fin. Blood vessels can be seen as cavities filled with red blood cells (red arrows). Nucleated fish red blood cells are stained bright red, pigment as brown, muscle tissue as brick red and connective tissue as turquoise.

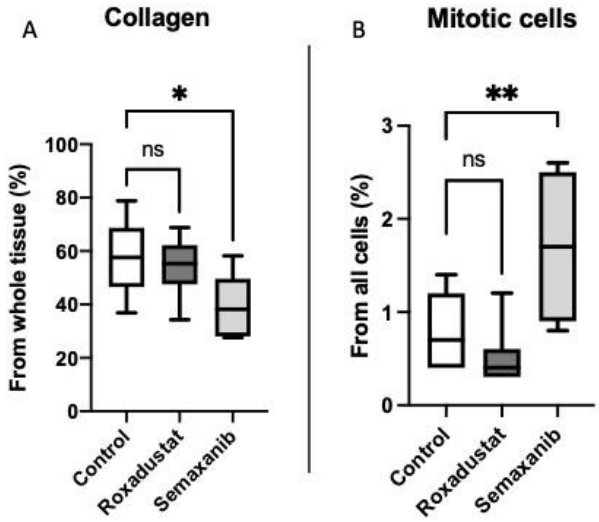


**Figure 9.** (A) The amount of collagen (%) from the whole tissue area in the caudal fin of turquoise killifish strain MZCS222. The amount of collagen was statistically lower (**p* = 0.0387) in semaxanib group when compared to control group after 8-day treatment (n=6-7/group). No significant effects of roxadustat on the amount of collagen in caudal fin were observed. (B) Mitotic cells (%) from all cells in the caudal fin of turquoise killifish strain MZCS222. No significant effects of roxadustat on mitotic cells in caudal fin were observed, but in semaxanib group the number of mitotic cells was significantly higher (***p* = 0.005) than in control group (n=7/group). The results were statistically analyzed using one-way ANOVA followed by Dunnett's multiple comparisons test. A *p* value of < 0.05 was considered significant.

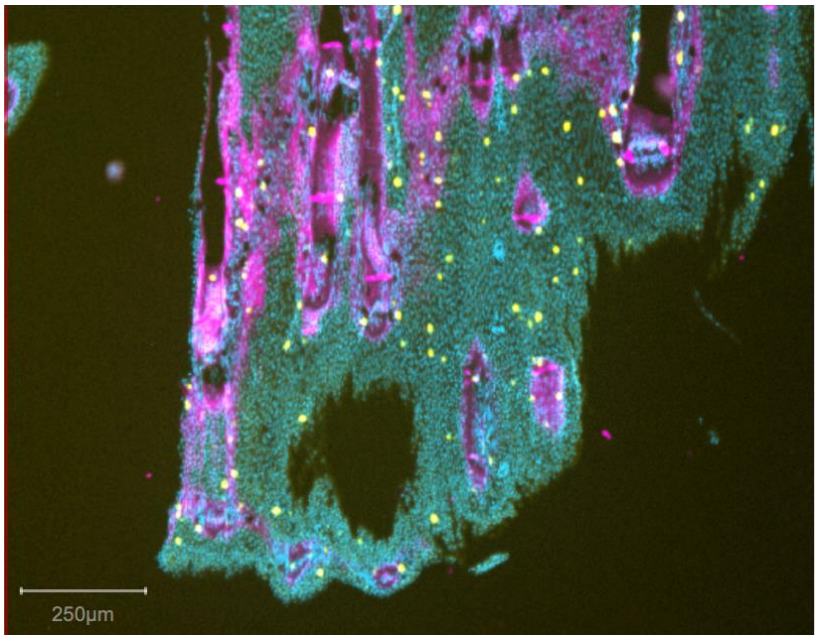


**Figure 10.** An example of PHH3 & CNA35 double staining. Antibody for PHH3 stains the mitotic cells (yellow dots) during chromatin condensation at mitosis. CNA35 stains the collagen (purple) in the tissue. DAPI was used as a nuclear stain (blue/turquoise).

Due to challenges in analyzing blood vessels from small samples, embedding fin pieces on a transverse plane was tried with three samples. These samples were sectioned and stained with hematoxylin and eosin (figure 11). The quality of the staining was good, and the structure of the fin was clearly visible. However, unfortunately hardly any red blood cells were identified from the sections, and thus, calculating blood vessels was not possible.

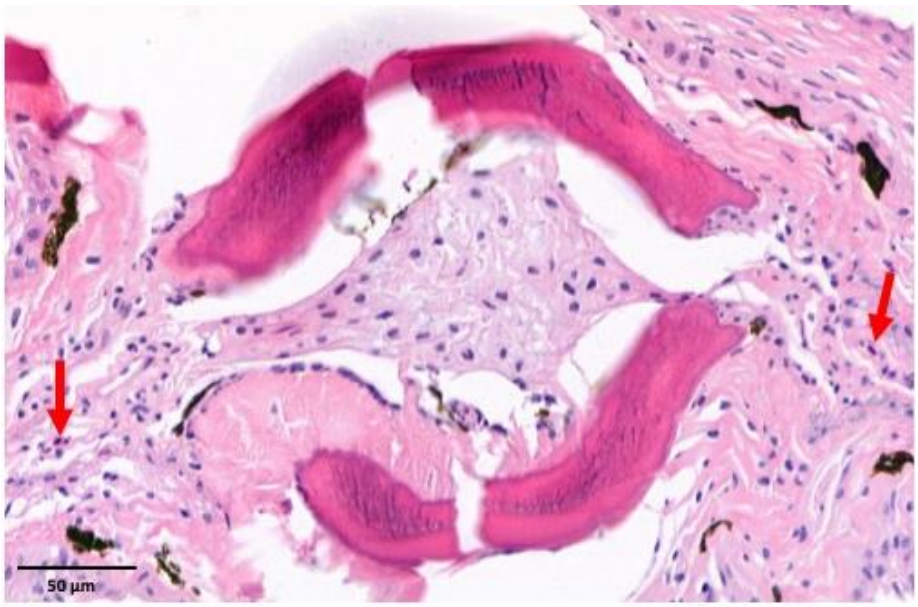


**Figure 11.** A piece of caudal fin embedded on a transverse plane and stained with hematoxylin and eosin. Red arrows indicate nucleated red blood cells in fish.

### 2.2.3 Gene expression analyses from young and middle-aged fish

The differences in the wound healing of caudal fin between young (5 weeks) and middle-aged (12 weeks) turquoise killifish strain MZCS222 were investigated from the caudal fin tissue samples collected in a previous study by Kosonen (2020). To investigate possible angiogenesis-related changes during the regeneration of caudal fin at study days 0 (D0) and 8 (D8), the expression of *cd34* and *vegfa* were analyzed in the present study. These differences were also analyzed between young and middle-aged fish. The results are presented as relative quantification values, and *tbp* was used as a normalization gene. Water was used as a negative control and four replicates per sample were applied. In *cd34,* no statistical differences were observed between young and middle-aged fish at D0 or D8 (figure 12A). In addition, the expression of *cd34* did not statistically differ between D0 and D8 in young or in middle-aged fish. No differences were either observed in the expression of *vegfa* between young and middle-aged fish at D0 (figure 12B). In addition, the expression of *vegfa* did not differ statistically in middle-aged fish between D0 and D8. However, in young fish the expression of *vegfa* was higher ($p = 0.0007$) at D8 than in D0. In addition, the expression of *vegfa* in young fish was higher ($p = 0.0009$) at D8 than in middle-aged fish.

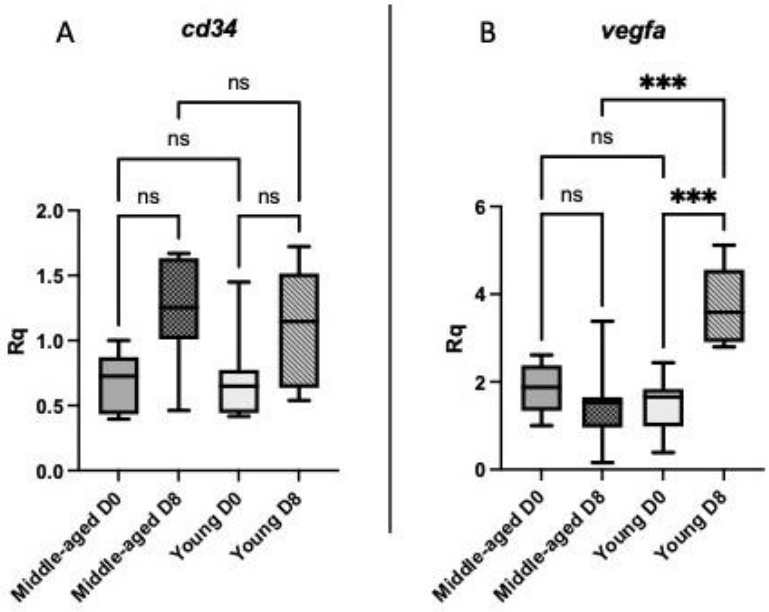


**Figure 12.** Gene expression of (A) *cd34* and (B) *vegfa* in the caudal fin of young and middle-aged turquoise killifish strain MZCS222 before and after 8-day wound healing study. (A) In *cd34,* no statistical differences between young and old fish at the baseline at D0 were observed (n=7/group). In addition, the expression of *cd34* did not statistically differ between D0 and D8 or after 8-day wound healing study between young and middle-aged killifish. (B) No differences in the expression of *vegfa* were observed between young and middle-aged fish at D0 (n=6-8/group). In addition, the expression of *vegfa* did not differ statistically in middle-aged fish between D0 and D8. However, in young fish the expression of *vegfa* was higher (***$p$ = 0.0007) at D8 than in D0. In addition, the expression of *vegfa* was higher (***$p$ = 0.0009) at D8 in young fish when compared to middle-aged fish. Statistical analyses were performed using two-way ANOVA followed by Šidák's multiple comparisons test. A $p$ value of $< 0.05$ was considered significant.

## 2.3 Wound healing studies with zebrafish

### 2.3.1 Growth length analyses from young and old fish

Differences in wound healing between young (4 months) and old (40 months) male zebrafish were investigated by following the regeneration of caudal fin for 8 days. At D0, a piece of caudal fin was amputated, and the fin was photographed at D0, D2, D4, D6 and D8. The length of the regenerated part of the fin was measured in millimeters in Fiji image analysis software (Schindelin et al., 2012) both from the ventral and the dorsal side of the fin. Then, the mean value of these two lengths was calculated as percentages from the length of the amputated part of the fin at study day 0. The results from the study showed that in old fish the regeneration of the caudal fin is significantly impaired at D8 ($p$ = 0.0004, figure 13) when compared to young fish. The trend towards this can be seen

already at earlier time points, and for instance at D6 the *p* value is nearly significant being 0.0596. The regeneration of the fin was already observed at D2 with the mean values of 4 % in growth length for young fish and 1 % for old fish. At D8, the means of the growth lengths were 26 % and 7 %, respectively. The growth rate was approximately 3 % per day in young and 1 % in old fish. Representative images of the regeneration during the study are presented as an example in figure 14.

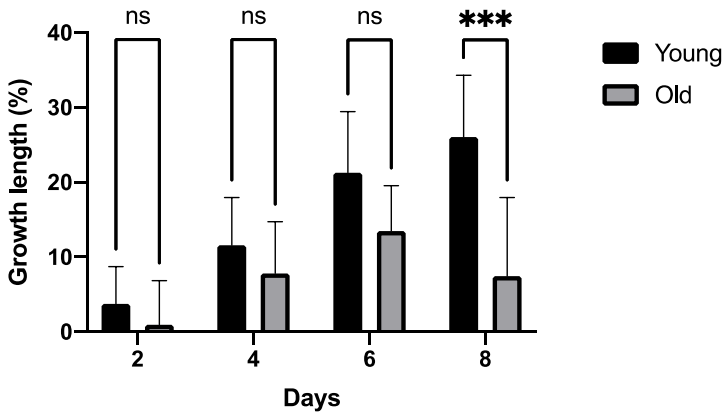


**Figure 13.** The growth length (%) of zebrafish caudal fin between young and old zebrafish during 8-day wound healing study. Statistical difference in growth length between young and old zebrafish is significant at D8 (****p* = 0.0004), n=12/age/timepoint). Bars represent means with SD. Statistical analyses were performed using two-way ANOVA followed by Šidák's multiple comparisons test. A *p* value of < 0.05 was considered significant.

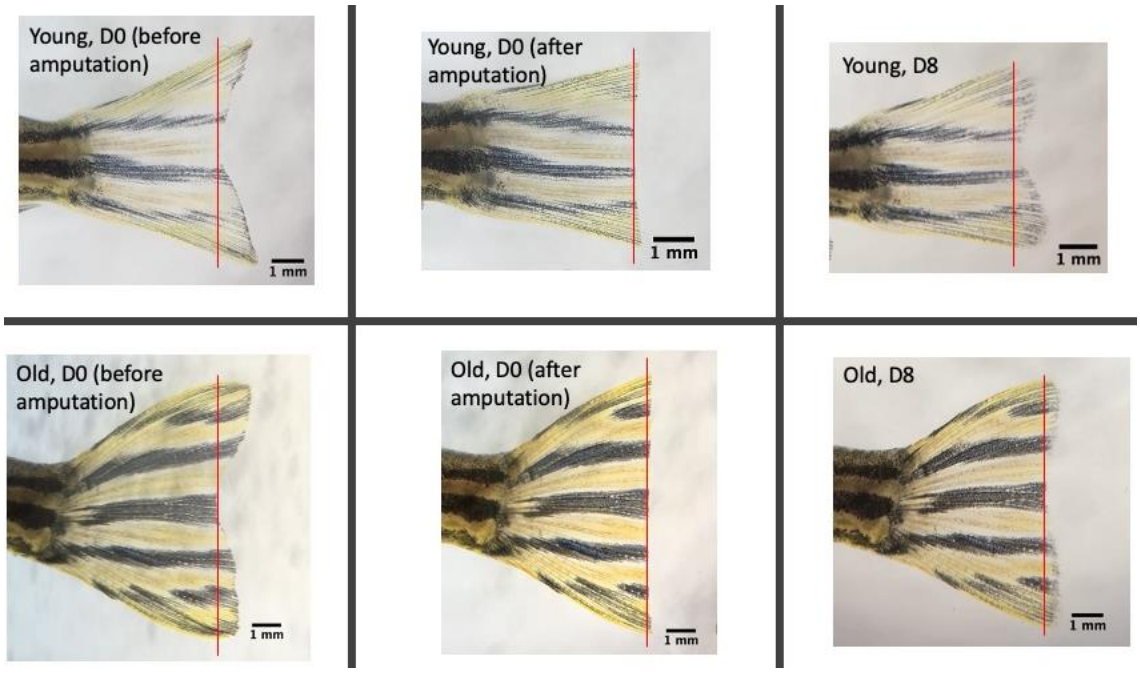


**Figure 14.** An example of the regeneration of the caudal fin in young (4 months) and old (40 months) zebrafish during 8-day wound healing study. Red line indicates the point for caudal fin amputation.

In order to evaluate if there are any differences in the regeneration between the dorsal and the ventral side of caudal fin, the growth lengths between the sides were compared both in young and in old fish (figure 15). Statistically significant differences in the growth length between the dorsal and the ventral side of the fin were not observed in young or in old zebrafish.

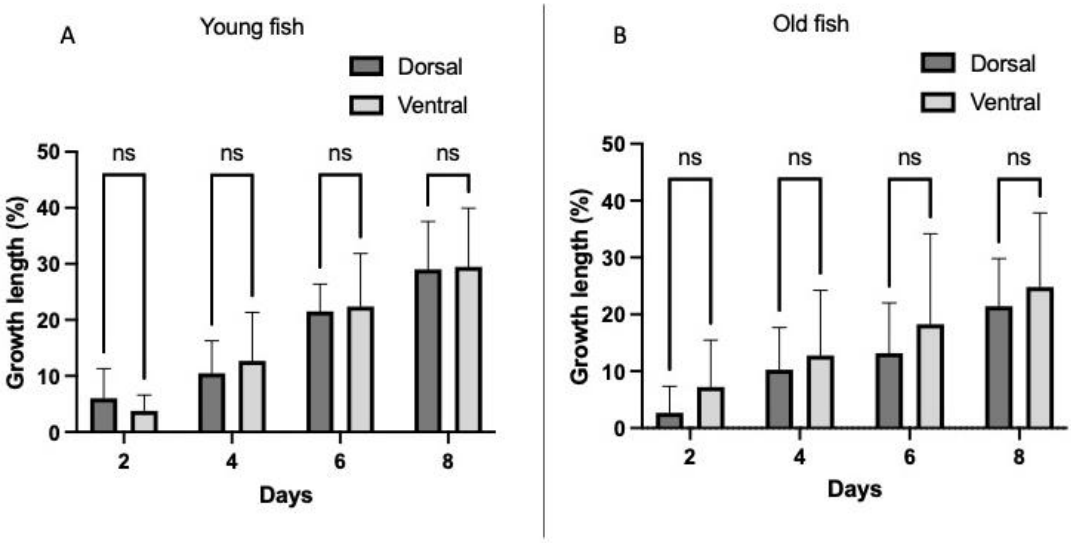


**Figure 15.** The growth length (%) in the dorsal and in the ventral side of the caudal fin in (A) young and (B) old zebrafish during 8-day wound healing study (n=12/side/timepoint). No statistical differences in the growth length between the dorsal and the ventral side of the fin were observed in young or in old zebrafish. Bars represent means with SD. Statistical analyses were performed using two-way ANOVA. A $p$ value of $< 0.05$ was considered significant.

### 2.3.2 Growth length analyses from the drug study with larval fish

The effects of chosen angiogenic (sodium nitroprusside, tazarotene, roxadustat, deferoxamine and cobalt chloride) or antiangiogenic (semaxanib) drugs on the wound healing of larval zebrafish *Tg(fli:EGFP*) caudal fin were investigated in a 48-hour drug study. Prior to the treatment, at 2 days post fertilization (dpf) a piece of caudal fin was amputated, after which the drug treatment was started. The caudal fin was imaged before and after the 48-hour treatment, and its length was measured in Fiji image analysis software (Schindelin et al., 2012). The length of the regenerated fin was calculated as percentages from a mean total caudal fin length of the uncut control larvae at 4 dpf. For comparing the drug effects also untreated control group with caudal fin amputation was used. The results showed that the regeneration of the caudal fin was impaired with 10 µM

semaxanib concentration ($p < 0.0001$), but not with the lower doses of 0.1 and 1 µM (figure 16A). No improvement on regeneration was seen with sodium nitroprusside (figure 16B), deferoxamine (figure 17B) or cobalt chloride (17C). Tazarotene was toxic to larvae with all the used concentrations. Due to toxicity the caudal fins of the larvae even shrunk ($p < 0.0001$, figure 16C). Toxicity was also observed with roxadustat. Almost all the larvae were lost in the roxadustat groups with the two highest concentrations of 15 µM and 50 µM. Toxicity was clearly seen also in the group with the lowest dose (2.5 µM) in which the growth length of the caudal fin was impaired significantly ($p = 0.0008$) when compared to control group (figure 17A). Representative images of the regeneration of the caudal during the 48-hour study and the toxic effects of tazarotene and roxadustat are presented as examples in figures 18 and 19.

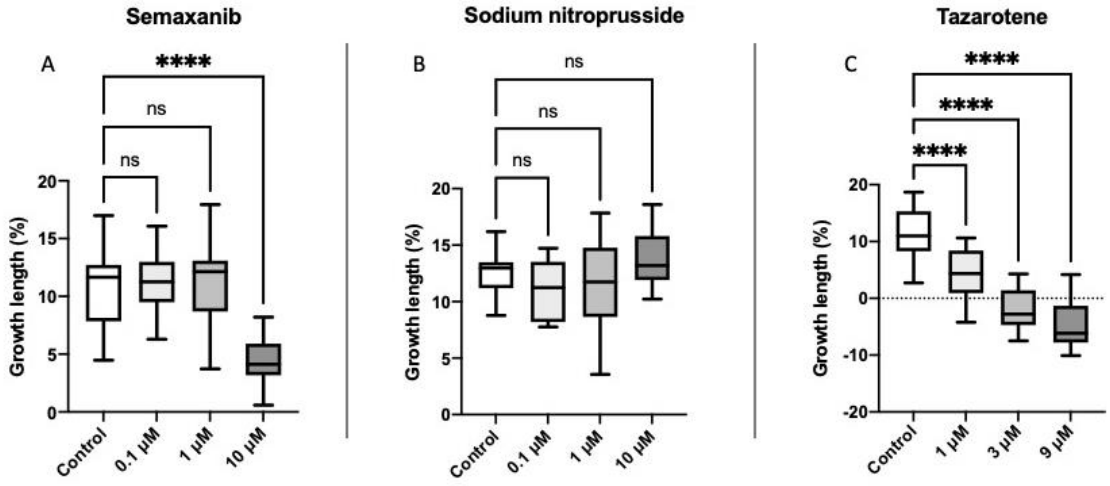


**Figure 16.** The growth length (%) of the larval zebrafish caudal fin treated with semaxanib, sodium nitroprusside or tazarotene. (A) The regeneration of the caudal fin was impaired by with 10 µM semaxanib concentration (****$p < 0.0001$, n=18-20 in all groups). (B) With sodium nitroprusside no statistically significant effects on the growth length of the caudal fin were observed with any of the doses (n=12-13/group). (C) Tazarotene was toxic with all the used concentrations. Due to toxicity the caudal fins of the larvae even shrunk, which can be seen as negative values in growth lengths (****$p <$ 0.0001, n=19-20/group). The results were statistically analyzed using one-way ANOVA followed by Dunnett's multiple comparisons test. A $p$ value of < 0.05 was considered significant.

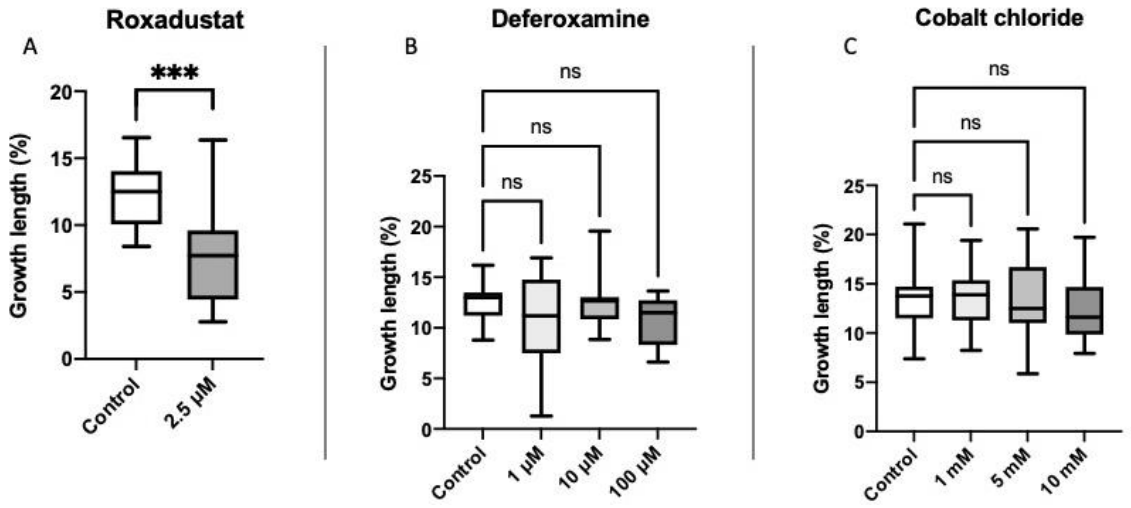


**Figure 17.** The growth length (%) of the larval zebrafish caudal fin treated with roxadustat, deferoxamine or cobalt chloride. (A) Toxicity was clearly seen in the roxadustat group with the lowest dose in which the growth length of the caudal fin was impaired significantly (***$p$ = 0.0008) when compared to control group (n=14 in all groups). (B) Deferoxamine showed no statistically significant effects on the caudal fin regeneration (n=12-13/group). (C) With cobalt chloride no effects were either seen, except for some toxicity in the group with the highest concentration in which 6 larvae were lost (n=17-18 in all groups). The results were statistically analyzed using one-way ANOVA followed by Dunnett's multiple comparisons test. A $p$ value of $< 0.05$ was considered significant.

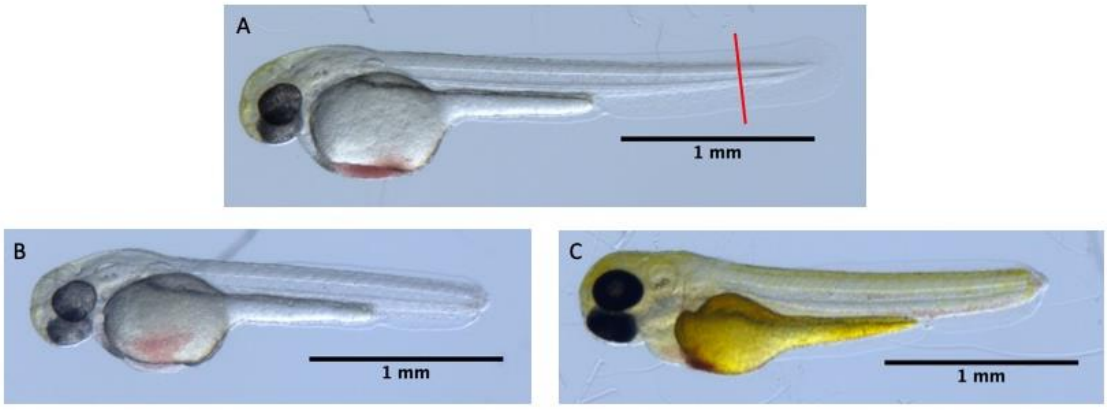


**Figure 18.** Larval zebrafish in semaxanib group during 48-hour wound healing study. (A) Larval zebrafish *Tg(fli:EGFP)* at 2 dpf before caudal fin amputation. The point for amputation is marked with red line. (B) Larval zebrafish after caudal fin amputation at 2 dpf. (C) Larval zebrafish at 4 dpf treated with 10 µM semaxanib for 48 hours. The larva has stained yellow due to the yellowish color of semaxanib.

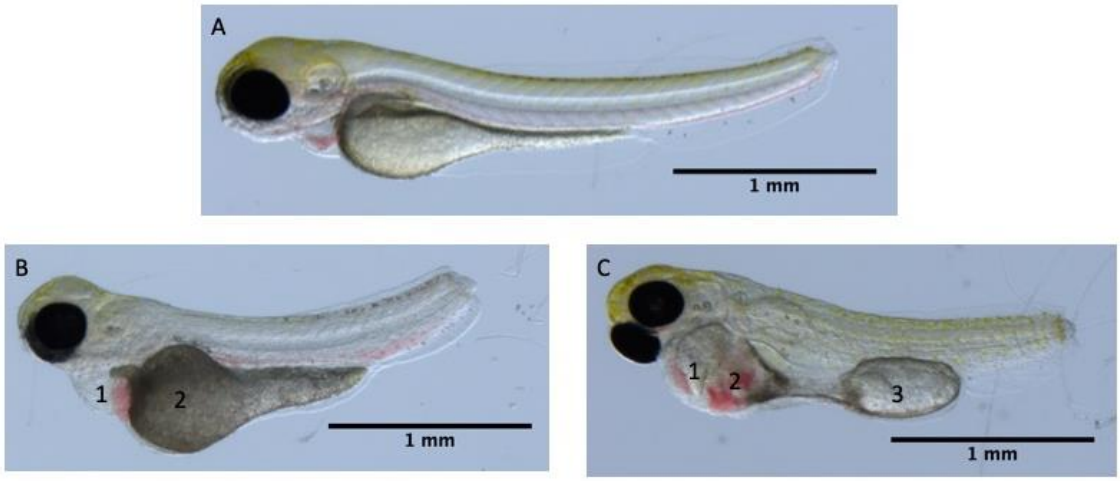


**Figure 19.** Toxic effects of tazarotene and roxadustat in larval zebrafish during 48-hour wound healing study. The toxic effects of (B) 9 µM tazarotene dose and (C) 15 µM roxadustat dose are clearly visible in the images taken after the 48-hour treatment when compared to (A) untreated control group. Developmental deformities can be seen for instance in (1) the heart area, (2) yolk sac and (3) intestine. Also, liver situated behind the yolk sac may be affected.

# 3. Discussion

## 3.1 Laboratory set-up of turquoise killifish strain GRZ

Due to challenges in setting up a fast-aging turquoise killifish strain GRZ in laboratory, wound healing studies with GRZ were not possible. These challenges were most likely due to several different things. The breeding experiments were carried out based on earlier experience in raising turquoise killifish strain MZCS222 and by modifying the protocols of Dodzian et al. (2018) and Polačik et al. (2016). In the first hatching experiment, the diapausal eggs received from Czech Academy of Science had been stored in dry peat at room temperature for several months. The exact number of embryos in the peat was unclear as it was difficult to see all the embryos covered in peat, but only 6 fish were obtained from the first hatching experiment. As it is known that unsynchronous development in annual fish is common (Wourms et al., 1972), it is possible that variable number of undeveloped eggs remained in the wettened peat after hatching. In later hatching experiments, altogether 4 embryos were obtained. Problems related to those experiments are discussed later.

Following hatching, the juvenile fish in the present study were fed with *Artemia* for the first days 2-3 times per day, after which habituation to blood worms was started as the fish grew. The feeding with blood worms was narrowed down to once daily 2 weeks post hatching. However, according to protocols by Dodzian et al. (2018) and Polačik et al. (2016) the energy demand in turquoise killifish is high and the fish should be fed at least twice daily. Especially in order to obtain successful egg production, feeding with high quality cultured bloodworms, such as Hikari, is recommended (Polačik et al., 2016). After facing challenges in egg production in the present study, twice daily feeding with blood worms was continued, and the egg production was clearly increased. As there is no standardized diet available for laboratory breeding of turquoise killifish (Žak et al., 2020), the selection of high-quality food is difficult. Turquoise killifish is reluctant to eat dry food complicating its feeding in laboratory conditions (Polačik et al., 2016). The problems associated with the use of blood worms are due to the variability in the quality of blood worms between suppliers (Dodzian et al., 2018; Polačik et al., 2016). Especially when performing aging studies, the use of standardized diet is a prerequisite (Liang et al., 2018). Although not totally optimal yet, the standardization of the killifish diet is taking

important steps. For instance, Žak et al. (2020) tested a pelleted diet in turquoise killifish and observed that this dry food was well accepted by the fish at 21 days post hatching.

Even though the effect of twice daily feeding on egg production in the present study was clear, the number of eggs was still not optimal, and problems in the incubation of fertilized eggs were also faced. A plastic box with sand substrate to trigger spawning finally resolved the problems related to egg production, and even several tens of fertilized eggs per day were obtained. In the protocol by Dodzian et al. (2018) the use of sand substrate is also recommended, and Polačik et al. (2016) recommends glass beads as a substrate for spawning.

During egg incubation, some contamination issues were observed. Adding methylene blue and gentamicin to the incubation wells prevented bacterial growth, but challenges were still faced. For instance, many of the fertilized eggs decayed within few days after the start of the incubation. Incubating eggs in peat instead of water is also possible and mimics natural conditions better than water. However, incubation in water allows more careful observation and control of the embryo development in detail. (Dodzian et al., 2018) In the present study only incubation in water was tested, and therefore, incubation in peat should be tested in the future studies to compare the incubation success between these methods.

The constant use of methylene blue and gentamicin during embryo incubation could have also caused developmental issues on fish embryos. No studies concerning the effects of methylene blue on the development of turquoise killifish has been done, but studies with zebrafish embryos/larvae have been performed for instance by Hedge and Sanders (2017). They observed no developmental issues with concentrations ranging from 0.624 to 10 µM after incubating embryos/larvae in methylene blue from 0 to 4 dpf. However, in the present study larvae were treated with 0.624 µM methylene blue for several weeks. Gentamicin is known to cause ototoxicity (Ton and Parng, 2005; Owens et al., 2009), oculotoxicity (Deeti et al., 2014) and behavioral changes (Han et al., 2020) in zebrafish embryos and larvae with concentrations ranging from 0.1 to 400 µM. The used exposure times in earlier studies have been 24-48 hours. The dose used in the present study was 2 µM, but the exposure times were up to several weeks, similarly as with methylene blue.

In later hatching experiments, some embryos/fish were lost due to unknown reasons during hatching. Immediate onset for feeding after hatching is important with turquoise killifish (Polačik et al., 2016). *Artemia* was provided to hatching fish at the start of the hatching experiment and at least twice after that during the same day. However, the fish were not fed late in the evening causing delays up to 17 hours in the feeding between the afternoon and next morning. This may have been problematic, if some of the eggs were hatched late in the evening with no possibility for immediate eating. *Artemia* can live only for some hours in fresh water (Brine Shrimp Direct, 2021).

In the protocol by Dodzian et al. (2018) it is recommended that incubation of ready-to-hatch embryos should not be prolonged more than two weeks, as the viability of the embryos will decrease. It is possible that in the present study some of the embryos were already overdue at the time of hatching. Poor success in obtaining sensible amounts of ready-to-hatch embryos created problems in synchronized hatching as the eggs had to be collected during several weeks.

Even though only 10 turquoise killifish of strain GRZ were successfully bred in the present study, a small survival analysis was done. Based on the survival analysis, a median lifespan of 14 weeks in GRZ was reported (range 12-21 weeks). Terzibasi et al. (2008) reported in GRZ a median lifespan of 9 weeks with maximum lifespan of 12 weeks. This variability clearly indicates differences between laboratories and in their environmental conditions. Decreasing water temperature from 25 to 22°C significantly lengthens the lifespan of turquoise killifish (Valenzano et al., 2006). Dietary restriction in GRZ has been shown to increase the median lifespan from 11.5 to 13 weeks (Terzibasi et al., 2009). In the present study, 6 out of 10 fish were fed with blood worms only once daily from age 2 to 8 weeks, which likely prolonged the median lifespan of GRZ.

When comparing the median age of GRZ to MZCS222 (33 weeks) in the present study, it was observed that the difference between the median lifespans of these strains was statistically significant ($p < 0.0001$). These results clearly indicate that the aging process in GRZ is faster than in MZCS222 making it a convenient and cost-effective strain for aging studies if the challenges in their breeding can be overcome.

## 3.2 Wound healing studies with turquoise killifish strain MZCS222

### 3.2.1 Gene expression analyses from young and middle-aged fish

In the study by Kosonen (2020), differences in the wound healing of caudal fin between young (5 weeks) and middle-aged (12 weeks) turquoise killifish strain MZCS222 were investigated in an 8-day study. In that study, the results showed that in middle-aged fish the regeneration of caudal fin was significantly impaired ($p < 0.001$) starting from study day 7 when compared to young fish. In order to investigate angiogenesis-related differences in the caudal fin before and after the wound healing study and between young and old fish, the expression of *cd34* and *vegfa* were analyzed in the present study.

CD34 is expressed on the filopodia of sprouting tip cells during active angiogenesis (Siemerink et al., 2012) and its role in tumor angiogenesis is especially well established. The role of CD34 in wound healing has been shown for instance by Qi et al. (2020). In their study, the treatment of diabetic ulcers in rats with tacrolimus resulted in mobilization of $CD34^+$ endothelial progenitor cells into the wound area and in improved microcirculation in diabetic feet. In addition, Lo et al. (2017) showed that CD34 has an important role in maintaining vascular integrity in lungs after tissue damage in mice. $CD34^+$ mononuclear cell therapy has even been tested in clinical trials for limb ischemia, but the results have been inconclusive so far (Pan et al., 2019). There is no data available about the possible role of CD34 in the wound healing of turquoise killifish. In the present study, no differences in the expression of *cd34* were observed when comparing the results between young and middle-aged fish or between D0 and D8. However, as it is known that angiogenesis during wound healing is impaired in elderly people, the involvement of CD34 in the process is possible. Earlier sampling timepoints would offer more data about the possible role of CD34 in the early stages of caudal fin regeneration.

VEGF is the key regulator of angiogenesis (Ferrara, 2004). Mechanical injury provokes its upregulation via hypoxia on wounded skin. Increased levels of VEGF become normalized in the later wound healing stages as the angiogenesis subsides. (Brown et al., 2002) In the present study, the results from the gene expression analyses showed that the expression on *vegfa* was significantly higher ($p < 0.0007$) in young fish at D8 when compared to D0. Furthermore, the expression of *vegfa* was also higher ($p = 0.0009$) at D8

in young fish when compared to middle-aged fish. In middle-aged fish, no differences were observed between D0 and D8. These results indicate that in young turquoise killifish the expression of *vegfa* increases during 8-day regeneration, but not in middle-aged fish. This finding is in line with the observation by Kosonen (2020) that blood vessel density was significantly higher in young fish at D8 when compared to middle-aged fish. In humans, it is known that low levels of VEGF are associated to chronic wounds and aging-related decline in wound healing. Complications in wound vascularization due to decline in VEGF production seems to contribute to the delay in healing process. (Johnson and Wilgus, 2014) Based on the present study, VEGF has a significant role in wound healing related angiogenesis also in turquoise killifish.

### 3.2.2 Gene expression analyses from the drug study

Gene expression analyses were performed in the present study from the samples collected by Kosonen (2020) from a wound healing study with drug treatment with turquoise killifish strain MZCS222. In the study by Kosonen (2020), old, 32-week-old turquoise killifish were treated with angiogenic compound roxadustat or antiangiogenic compound semaxanib for 8 days after caudal fin amputation. Treatment with semaxanib resulted in decline ($p < 0.001$) in the growth length already at D6, but no statistically significant effects were seen with roxadustat when compared to control group. However, at D8 the there was a significant increase ($p < 0.01$) in the growth rate of caudal fin in roxadustat group. (Kosonen, 2020) In order to further elucidate the effects of roxadustat and semaxanib on the gene expression in the regenerated caudal fin, analyses for *vegfa*, *cd34, tie1* and *vcam1* were performed in the present study. There is no previous data available from turquoise killifish wound healing studies concerning the effects of roxadustat and semaxanib on gene expression analyses selected for the study.

The results in the present study showed that in the fish treated with semaxanib the expression of *cd34* was lower ($p = 0.0103$) than in non-treated control group at D8. As no differences in the expression of *cd34* were observed in the wound healing between young and middle-aged turquoise killifish, the results from the drug study suggest that the lowered expression of *cd34* could be related to the inhibitory effect of semaxanib on fin regeneration. In order to evaluate the role of CD34 in the angiogenesis during the

wound healing of turquoise killifish more detailed further studies should performed, especially regarding the expression of *cd34* in old fish.

Based on the results from the present study, there were signs of lowered expression levels of *vegfa* by semaxanib when compared control group, but this finding was not statistically significant ($p$ = 0.0528), however. The reason why the effect of semaxanib on the expression of *vegfa* was not clear could be due to the sampling timepoint of the regenerated piece of fin. It is possible that the lowest expression level at the time of fin sampling at D8 had already passed. However, as the expression level was close to significant, repetitive studies with semaxanib and possibly with other VEGFR inhibitors would be valuable. Especially analyzing *vegfa* levels from different timepoints after wounding would provide more information about the changes in the gene expression on the course of regeneration. VEGFR inhibitors could be also tested for wound healing in younger fish in order to see if the expression levels of *vegfa* are affected accordingly.

No statistically significant effects of semaxanib or roxadustat were seen in the expression of *tie1* in the present study. Tie1 is expressed on endothelial cells and its deletion has been shown to inhibit angiogenesis (D'Amico et al., 2014). As an orphan receptor, the effects of Tie1 on angiogenesis are exerted via Ang1/Tie2 signaling (Savant et al., 2015). The expression of Tie1 is induced by VEGF and hypoxia (McCarthy et al., 1998), and it has even been suggested as a potential target for anti-angiogenic treatments (D'Amico et al., 2014). In a study by Korhonen et al. (1992), it was observed that during neovascularization of mouse ovarial stroma, Tie expression was increased 3 days post wounding and reached the maximum level at day 7 post wounding in newly formed blood vessels of granulation tissue. At day 14, the expression had reverted to a lower level observed at day 2 (Korhonen et al., 1992). In the light of these findings, it is possible that in the present study the wound healing in turquoise killifish had already passed the time frame for increased *tie1* expression at the time of fin sampling. As no clear effects of semaxanib or roxadustat on *vegfa* were observed, it is possible that this result has further affected also on *tie1* expression.

The results from the present study showed that the expression of *vcam1* was not affected by the treatment with semaxanib or roxadustat. The expression of VCAM-1 is especially related to the development of different malignant tumors (Chen et al., 2011; Huang et al.,

2013), but it is also involved in the progression of several inflammatory diseases (Wang et al., 2015; Agassandian et al., 2015). VCAM-1 is mainly expressed on vascular endothelial cells upon activation (Rice and Bevilacqua, 1989) by inflammatory factors, such as TNF-α, but also by ROS, shear stress (Cook-Mills et al., 2011) and VEGF (Fearnley et al., 2014; Kim et al., 2001). In a study by Dreßler et al. (1999), the age of human skin wound was evaluated by comparing the expression of VCAM-1 between uninjured and injured skin using immunohistochemistry. In injured skin, the staining reaction for VCAM-1 was positive 3 hours after injury lasting up to 3.5 days post injury. (Dreßler et al., 1999) This and the other mentioned studies suggest that VCAM-1 expression peaks during the inflammatory phase of wound healing. Due to the early expression of VCAM-1 during wound healing process it is likely that the regeneration of caudal fin in turquoise killifish had already passed the inflammatory phase and reached the later phases of repair. However, it is difficult to speculate the results due to the low number of samples, especially in roxadustat group, in which there were many samples in which the expression of *vcam1* was under detectable levels. In order to evaluate the significance of *vcam1* during the regeneration process in turquoise killifish, gene expression analyses should be performed from different timepoints during the caudal fin regeneration.

### 3.2.3 Histological analyses from the drug study

In order to investigate the tissue level effects of the chosen drugs on the regeneration of caudal fin, blood vessel density was analyzed from the regenerated caudal fin samples collected from the drug study by Kosonen (2020). As the inhibitory effect of semaxanib on fin regeneration was seen as a decline in growth length in addition to reduced expression of *cd34* and amount of collagen in the fin tissue, it would have been presumable to find indications of this also in the blood vessel analysis. However, no statistical differences were observed in semaxanib or in roxadustat group when comparing the blood vessel density to control group. This result may be biologically relevant, or it may relate to the quality of the tissue sections. The tissue sections stained with MG were challenging to analyze due to the small size and irregular shape of the fin pieces. The samples were also partly transparent and very flexible complicating their embedding in paraffin. Therefore, some of the embedded samples were not in the desired frontal plane. Based on these difficulties, it was decided to try different orientation of the

fin pieces in paraffin embedding. The samples were embedded to paraffin on a transverse plane and stained with hematoxylin and eosin. Unfortunately, recognizing blood vessels was challenging also from these samples as there were hardly any red blood cells seen in the blood vessel cavities. One option to identify blood vessels from transverse sections would be to perform immunohistochemistry with endothelial markers, such as CD34 or CD31. Also, other analysis methods, such as imaging would be valuable. For instance, transparent turquoise killifish strains are under development (Krug, 2021). Optical transparency would enable GFP imaging of proliferating or migrating cells and blood vessels in transgenic fish.

The effects of roxadustat and semaxanib on cell proliferation in the regenerated caudal fin was analyzed from the tissue sections stained with PHH3 antibody. Phosphorylation of histone H3 takes place during the chromatin condensation at mitosis (Hans and Dimitrov, 2001). Especially the phosphorylation of histone H3 at the residue of serine 10 is crucial for the onset of mitosis (Nechiporuk and Keating, 2002). Thus, PHH3 antibody was used for staining mitotic cells in the tissue. The results from the analysis of PHH3 staining in the present study were very interesting as the treatment with semaxanib seemed to increase the number of mitotic cells in the tissue when compared to control group ($p$ = 0.005). Sakao and Tatsumi (2011) investigated the mechanisms behind neointimal changes of severe angioproliferative pulmonary hypertension in adult rats caused by the combination of hypoxia and semaxanib. They hypothesized that in response to the defects in survival signaling by apoptotic cells, conditions that favor hyperproliferative, apoptosis-resistant endothelial cells are created (Sakao and Tatsumi, 2011). This hypothesis could also explain the results from the present study: In response to hypoxia caused by the amputation and the treatment with semaxanib, endothelial cells in the regenerating caudal fin start to become apoptosis-resistant over time resulting in hyperproliferation. This being said, further studies with higher number of fish per group are needed in order to understand the tissue level changes during fin regeneration. In addition, TUNEL staining for detecting apoptotic cells in the tissue could provide more information about the interaction of the cells in the regenerating fin during and after the drug treatment.

To investigate the effects of roxadustat and semaxanib on collagen formation during caudal fin regeneration, CNA35 staining was performed. CNA35 is a recombinant

collagen probe designed for imaging collagen in the tissue (Aper et al., 2014). The results from the present study showed that the amount of collagen in the regenerated caudal fin was significantly declined in semaxanib group ($p = 0.0387$) when compared to the control group confirming the inhibitory effect of semaxanib on caudal fin regeneration. When angiogenesis is inhibited, the later phases of wound healing are also affected resulting in decreased formation of collagen. Thus, the results from the present study indicate that the regeneration was already in the later phases. With roxadustat, no differences in the regenerated caudal fin stained with PHH3 antibody and CNA35 collagen probe were observed when compared to control group. This is likely due to the overall modest effect of roxadustat on the regeneration of caudal fin.

### 3.2.4 Administration of the drugs

In the drug study by Kosonen (2020), the administration of the drugs to the fish was performed by diluting them in the tank water. This was done daily into fresh water in order to keep the tank water clean and to prevent the decay of the drugs in the water. The administration of drugs to fish is challenging, especially in the case of small fish. Therefore, the use of several administration techniques commonly used with rodents, such as oral or intraperitoneal, is limited with fish and often require anesthesia. Also, repeated intraperitoneal injections in fish may lead to infection or injury. (Dang et al., 2016) In the study by Kosonen (2020), diluting the drug in the tank water was justified as it simulates the transdermal absorption of topically administered wound treatments in humans. As the effects of semaxanib on regeneration were observed with many parameters, the absorption of the drug was probably sufficient. However, it remains unclear if the absorption of roxadustat was optimal. More concentrations should be tested in the future in order to rule out the possibility for too low of a dose.

## 3.3 Wound healing studies with zebrafish

### 3.3.1 Wound healing study with young and old zebrafish

Adult zebrafish is able to regenerate its caudal fin within 14-28 days after amputation depending for instance on diet, water quality and temperature (Cardeira et al., 2016). Several studies suggest that aging does not affect the regenerative capacity in zebrafish

(Itou et al., 2012; Panetta et al., 2008), but some functional impairment in different organs, such as in heart have been seen (Itou et al., 2012; Gonzalez-Rosa et al., 2014). However, for instance Shao et al. (2011) observed a decline in the regenerative capacity of 18-month-old zebrafish in the later phases of regeneration. Anchelin et al. (2011) for their part showed that in 24-month-old zebrafish the growth rate in caudal fin after amputation is significantly lower than in younger (18 months and under) fish.

In the present study, the capacity of 4- and 40-month-old zebrafish to regenerate their caudal fin after amputation was investigated. A wound healing study was performed, in which the regeneration was followed for 8 days. It was observed that the growth length of caudal fin in 40-month-old fish was significantly impaired ($p < 0.0004$) starting at 8 dpa when compared to 4-month-old fish. There are no earlier studies concerning caudal fin regeneration in zebrafish as old as 40 months, but Itou et al. (2012) reported no decline in the regenerative capacity of 26 - 36-month-old zebrafish. The results from the present study are partly in line with those observed by Shao et al. (2011) with younger fish. In the present study the impairment in regeneration was observed already at 8 dpa whereas Shao et al. (2011) reported this decline starting from 20 dpa with 18-month-old zebrafish. Anchelin et al. (2011) also found that in 24-month-old zebrafish the decline was significant at 12 dpa when compared to younger fish. These findings suggest that the decline in the regeneration of caudal fin is associated with age and appears earlier during the regeneration process in old than in young fish. However, there seems to be no statistically significant differences in the regeneration between young and old zebrafish within the first days after amputation. This data proposes that the capability of zebrafish to initiate the process of regeneration is not impaired in 40-month-old fish but is significantly declined at around 8 dpa when the outgrowth of the fin is typically rapid. This phase is also characterized by the development of bone structures and pigmentation (Pfefferli and Jaźwińska, 2015).

In the present study, the decline observed at 8 dpa was especially interesting as it seemed that in old fish there was a slight decrease in the growth length from day 6 to day 8. This may be due to technical challenges in measuring the fin length or it may relate to the reshaping of the white excrescence during the outgrowth of the fin. In order to evaluate this more detailed, further studies with better imaging tools should be performed. The images taken with smart phone camera via microscope to image the caudal fin were

surprisingly good in quality, but especially measuring the transparent excrescence was challenging from some of the images.

In order to understand the mechanisms behind the decline in regenerative capability in old zebrafish, further analyses, such as gene expression analyses should be performed, especially from the timepoint when the decline was statistically significant. Also, studies continuing until full regeneration of caudal fin would be valuable in order to see if the decline still worsens over time.

### 3.3.2 Drug study with larval zebrafish

The effects of six different angiogenic or antiangiogenic compounds on the regeneration of larval zebrafish caudal fin were investigated in a 48-hour drug study. With angiogenic compounds tazarotene and roxadustat toxicity was observed with all doses. In roxadustat group, the used doses were 2.5, 15 and 50 µM. However, due to the lethal toxicity observed during the study, statistical analyses were possible only with the group with the dose of 2.5 µM. In this group, the decline in the regeneration of caudal fin was statistically significant ($p = 0.0008$). In the group that received 15 µM dose, toxicity was observed at least in the heart, yolk sac and intestine areas. The effect of roxadustat, inhibitor of HIF propyl hydroxylase, on the regeneration of larval zebrafish caudal fin has not been studied earlier. However, Jain et al. (2016) successfully used the dose of 2.5 µM for inducing hypoxia in zebrafish larvae. They treated larvae with roxadustat from 96 hpf until 102 hpf, which is much shorter than in the present study, in which the larvae were treated for 48 hours. Also, the initiation of the treatment was later in their study whereas in the present study roxadustat treatment was started at 48 hpf. Kim et al. (2020) used the doses of 15 and 50 µM in cell cultures for inducing hypoxia but treated cells only for 3 hours. Thus, it is possible that the doses used in the present study were too high and the length of the treatment was also too long. Instead of continuous exposure to roxadustat, shorter baths in drug water could be tested.

With retinoid acid agonist tazarotene toxicity was observed with all the selected doses (1, 3 and 9 µM) in a dose-response manner. The higher the dose, the more impairment in the caudal fin regeneration was seen. In all groups, this impairment was statistically significant ($p < 0.0001$). In addition, developmental deformities were visually observed

at least in the heart and yolk sac areas. The effects of tazarotene on the regeneration of larval zebrafish caudal fin has not been investigated earlier. However, the teratogenic effects of retinoids have been known for long and shown in several studies (Kistler et al., 1990; Bechter et al., 1992; Collins and Mao, 1999). In adult zebrafish, treatment with retinoid acid have been shown to cause teratogenicity in caudal fin after amputation, but not in pectoral fins (Géraudie et al., 2002). In addition, no improvement on fin regeneration were observed at least by Géraudie et al. (2002). However, due to the *in vitro* and *in vivo* potential of tazarotene in wound healing shown by Al Haj Zen et al. (2016) this compound could still be tested with lower doses in adult fish.

No effects with selected doses of 1, 10 ja 100 µM deferoxamine on zebrafish caudal fin regeneration were observed in the present study. Iron chelator deferoxamine has been used in several *in vitr*o and *in vivo* wound healing studies, but not in studies concerning the regeneration of larval zebrafish caudal fin. However, angiogenic effects of deferoxamine have been studied in larval zebrafish (Pawar et al., 2020). Pawar et al. (2020) used deferoxamine as an angiogenic control with concentrations of 25, 50, 100 ja 200 µM and reported a value of 55.8 µM as an effective concentration that is able to cause a change of 30 % in subintestinal vessels. Hamilton et al. (2014) for their part has reported a median lethal concentration of 1000 µM. Based on these findings, it is possible that in the present study the used concentrations were too low. One possibility is also that deferoxamine actually improved angiogenesis in zebrafish larvae, but not enough to affect caudal fin regeneration. The results in the present study may also be affected by the deterioration of deferoxamine in the 96-well plate during the 48-hour incubation at 28.5°C. It is stated in the product information sheet of deferoxamine that solutions deteriorate during storage and fresh solutions should be prepared upon usage (Product information sheet, Sigma-Aldrich, 2021), but in practice it is difficult to evaluate how fast does this deterioration progress at the incubation temperature.

Hypoxia-mimetic compound cobalt chloride has been widely used both in *in vitro* and *in vivo* research for investigating the effects of hypoxia at the molecular and cellular levels (Muñoz-Sánchez and Chánez-Cárdenas, 2019). In the caudal fin of adult zebrafish, cobalt chloride has been shown to increase blood vessel formation and accelerate regeneration (Eyries et al., 2008: Sagayaraj and Malathi, 2017). For hydroxylase inhibition, dose as high as 10 mM is needed with zebrafish larvae, but this dose also causes off-target toxicity

(Saeedi Saravi et al., 2009). A dose of 5 mM was successfully used with larvae in order induce retinal neovascularization with low mortality (Wu et al. 2015). In the present study, no improvement on caudal fin regeneration was seen with any of the used doses (1, 5 and 10 mM). However, some toxicity was observed with the highest dose of 10 mM as 6 larvae in the group were lost. In order to see any possible effects of cobalt chloride on angiogenesis, the blood vessel density in the regenerated caudal fins should be analyzed. Even if effects on angiogenesis could have been seen, the treatment for 48 hours may have been too short to improve caudal fin regeneration.

NO donor sodium nitroprusside has been shown to accelerate the appearance of certain blood vessels in the trunk of zebrafish larvae (Pelster et al., 2005). The potential of many other NO donors in improving wound healing has been shown both *in vitro* (Bove et al., 2007) and *in vivo* (Witte et al., 2002), but sodium nitroprusside has not been tested earlier for the regeneration of larval zebrafish caudal fin. Based on the present study no effects with this drug were seen on the caudal fin regeneration in larvae. These results could be due to low doses (0.1, 1 and 10 µM) used in the study. For instance, Leite et al. (2012) used a dose of 1 mM for treating larvae aged 7 dpf for 4 hours. Sodium nitroprusside is a short-acting NO donor (Carreiro et al., 2009), thus it is possible that the effect of the drug in the present study was too short. With higher dose and by changing the incubation medium containing the drug to new at least once or twice during the study, some effects on regeneration could have been seen. It is also important to note that low levels of NO (<100 nM) have been shown to promote angiogenesis and cell proliferation *in vitro*, whereas high doses (>500 nM) have been reported cause cytotoxicity and apoptosis (Burke at el., 2013). Thus, careful dose titration is likely needed also with larval zebrafish.

The efficacy of antiangiogenic VEGFR inhibitor semaxanib on MDA-MB-231 breast cancer cells has been studied for instance in zebrafish xenografts (Nakayama and Makinoshima, 2020). In the present study the inhibitory effect of semaxanib on larval zebrafish caudal fin regeneration was statistically significant ($p < 0.0001$) with the highest dose of 10 µM, but not with the lower doses of 0.1 µM and 1 µM. These results indicate that more dose titration should be done in the future studies in order to find the lowest effective dose. In order to prove that the inhibitory effect of semaxanib was due to impaired angiogenesis and not to toxicity, further analyses should be also done. For instance, the blood vessels could be analyzed with fluorescence microscope as transgenic

*Tg(fli:EGFP)* zebrafish line was used in the study. In this transgenic line, the expression of GFP is driven by the endothelial marker *fli1*. The visualization of the vasculature in the regenerated caudal fin in zebrafish larvae would be valuable also with the other compounds used in the present study in order to see any effects on angiogenesis.

## 3.4 Conclusions

Impaired wound healing and the lack of effective treatments for chronic wounds are a significant, worldwide concern. Aging is considered as one of the biggest risk factors for chronic wounds. The lack of proper preclinical *in vivo* models for wound healing complicates drug development. Due to these facts, one of the aims of the present study was to investigate the mechanisms behind impaired wound healing during aging by setting up a wound healing model with fast-aging turquoise killifish strain GRZ. With its median lifespan of 14 weeks, GRZ provides an excellent and cost-effective tool for aging studies. However, several difficulties were faced when trying to set up this model, thus no wound healing experiments could be done with the strain. In order to eventually set-up a turquoise killifish GRZ strain in laboratory, many detailed modifications concerning breeding and egg incubation are needed.

Despite of the mentioned challenges, the impairment in wound healing due to aging was studied with turquoise killifish (strain MZCS222) and zebrafish. These fish species/strains are longer lived than turquoise killifish strain GRZ with their median lifespans of 33 weeks (MZCS222) and 3.5 years (zebrafish). Due to slow aging process, these species are not very convenient in the laboratory setting for aging studies, but they can still provide valuable data concerning aging-associated decline in the regeneration of caudal fin. Based on the present study, it was observed that aging impairs the regeneration of caudal fin in zebrafish, and previously Kosonen (2020) has shown this same decline in old turquoise killifish strain MZCS222. Thus, both of these fish species could be used as models for impaired wound healing. In killifish, the results from the present study suggest that the impaired regeneration of caudal fin could be linked to the decline in VEGF production and further on angiogenesis. Angiogenesis has a significant role in the wound healing process. VEGF as an inducer for angiogenesis has a substantial role in human wound healing and based on the results from the present study, also in turquoise killifish. However, further studies should be performed in order to understand the underlying

mechanisms behind the impaired regeneration in both turquoise killifish and zebrafish during the whole regeneration process.

The effects of several angiogenic and antiangiogenic compounds on the regeneration of adult turquoise killifish and larval zebrafish caudal fin were also investigated in the present study. With VEGFR inhibitor semaxanib, which was selected as an antiangiogenic control drug, a decline in caudal fin regeneration both in old turquoise killifish and larval zebrafish was seen. This finding suggests that semaxanib impairs the regeneration of caudal fin by affecting angiogenesis and consequently also the later phases of regeneration. However, it would be of great importance to find also an angiogenic control drug for wound healing studies as the effects of roxadustat remained modest in the present study. In turquoise killifish, a slight improvement on the caudal fin growth rate with roxadustat was observed by Kosonen (2020), but no supporting results were found from the gene expression analyses or from histology in the present study. Also, in the studies with zebrafish larvae, no improvement on caudal fin regeneration was seen with angiogenic compounds roxadustat, tazarotene, sodium nitroprusside, deferoxamine and cobalt chloride. These results are probably related to several things, such as drug concentrations, toxicity, possible deterioration of the drugs and the used model. Therefore, more investigation with angiogenic compounds in both larval and adult zebrafish and also in adult turquoise killifish is needed in order to further validate the wound healing models. After further validation, modeling wound healing for instance in fast-aging turquoise killifish GRZ could be a valuable tool to study aging-related decline in wound healing and to screen new, potential drugs for wound healing in the preclinical phase of drug development. This kind of fish model could potentially accelerate drug development by reducing the number of expensive and time-consuming rodent studies.

# 4. Materials and methods

## 4.1 Laboratory set-up of turquoise killifish strain GRZ

### 4.1.1 Raising juvenile fish

The diapausal eggs of turquoise killifish GRZ were received as a kind gift from Czech Academy of Science. The eggs had been stored in dry peat in plastic bags at room temperature several months. When the hatching of the eggs was started, one plastic bag containing peat and eggs was emptied into a 5 l glass tank and wettened with 2-3 liters of 15-17°C system water (pH 7.3-7.6, temperature 27°C ± 2, conductivity 230 µS ± 30) to trigger the hatching. In later hatching experiments, the embryos developed in the incubator were directly moved from incubator to hatching tank. The tank was moved to a warm room with the temperature of 26°C near heater and positioned to a 20-30° angle for allowing the hatched fish to fill their swim bladder in the shallow end of the tank. Also, oxygen tablets (Oxylette, Hobby) were added in the water (1 tablet/l) to aid the hatched fish to fill their swim bladders. Prior to hatching and additionally as soon as any signs of hatched fish were seen, the fish were fed with *Artemia salina.* The nauplii of *Artemia salina* is used for feeding juvenile fish. *Artemia* can survive in fresh water only for some hours, thus the feeding of the fish was done 2-3 times a day. The decapsulation protocol for *Artemia* is attached in appendix 1.

Three days after hatching the killifish were moved to a bigger 40 l tank with aeriation. Water heater was added to the tank for keeping the water temperature at 28°C. The faeces and uneaten *Artemia* were cleaned from the tank bottom 2-3 times a week and concurrently about 50% of the water was changed to fresh prewarmed system water. After 10 days, chopped blood worms (Akvarie Teknik) in addition to *Artemia* were provided to killifish for 5 days in order to habituate them to eat more nutritious food. After habituation, the fish were placed individually to 40 l tanks attached to circulating system water. Individual housing was used at first in order to prevent the fish from cannibalizing smaller fish in the same tank. Finally, the fish were group housed (2-4 fish per tank) to 60 l tanks 4-5 weeks post hatching and fed with bloodworms once or twice daily until their natural death.

### 4.1.2 Breeding

For breeding turquoise killifish strain GRZ, group spawning was started when the fish had reached sexual maturation, approximately 5 weeks post hatching. The spawning was initially tried in a 10 l glass tank filled with system water. A mesh was placed on the bottom of the tank for preventing the fish from cannibalizing the eggs. One male and two females were placed in the tank to avoid possible violent harassment by the male. The tank was placed overnight near the heater in a warm room with the temperature of 26°C. After overnight mating, the fish were placed back to their original tanks attached to circulating system water. The spawned eggs were collected by pouring and flushing the mating tank water through a tea sieve. The collected eggs were gently washed with system water on a petri dish to get rid of unwanted organic material, such as feces. After this, the eggs were checked under microscope for evaluating the fertilization. The fertilized eggs were placed on a clean petri dish filled with E3 medium containing 0.624 µM of methylene blue (Sigma-Aldrich) for preventing any bacterial growth and transferred into the incubator with the temperature of 28°C.

Due to poor success in spawning, the use of sand substrate as a trigger was tried. The sand (particle size 2-3 mm in diameter) was placed on a plastic box (figure 20) with dimensions of 8 cm (height) x 20 cm (length) x 10 cm (width), and the box was placed in the tanks of the fish. The box containing the sand was flushed with system water 2-4 times a week, and the eggs were collected by pouring the water from the sand box through a tea sieve, after which they were checked for fertilization.

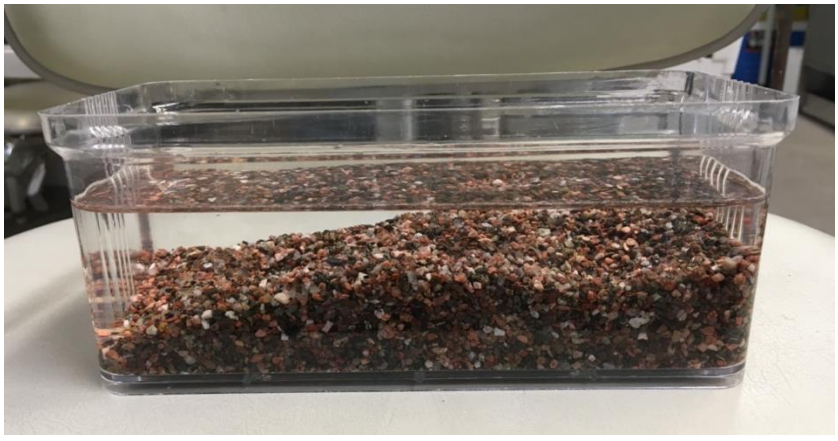

**Figure 20.** Plastic box used for spawning containing system water and sand substrate.

### 4.1.3 Incubation of eggs

The development of the fertilized eggs was checked under stereomicroscope regularly every 2-4 days until the eggs reached ready-to-hatch state. E3 incubation medium containing 0.624 µM of methylene blue was changed to new 2-3 times per week. As the survival of the eggs in the incubator was challenging due to contaminations and some other unknown reasons, the petri dish was changed to a 24-well plate for individual incubation of eggs. Also, to avoid bacterial growth in the wells, gentamicin (Sigma-Aldrich) was added to E3 medium containing methylene blue for obtaining final gentamicin concentration of 2 µM. The fertilized embryos reached ready-to-hatch state approximately in 15-18 days. As a sign of this, gold-pigmented irises were clearly visible. After reaching ready-to-hatch state, the embryos were kept in the incubator for 1-30 days before hatching was started.

## 4.2 Wound healing studies with turquoise killifish strain MZCS222

### 4.2.1 Preparation of cDNA

RNA samples from turquoise killifish MZCS222 caudal fin had been collected in 2020 from the drug study by Kosonen (2020). In addition, RNA samples were collected from the study in which the wound healing between young and middle-aged killifish were compared. The extracted RNA was stored at -80ºC for reverse transcription. The High-Capacity cDNA Reverse Transcription Kit (Applied Biosystems) was used for the conversion of extracted RNA to single-stranded cDNA, and the reverse transcription was performed according to manufacturer's protocol. Either 100 ng or 200 ng of RNA was converted to cDNA. The total reaction volume prepared was 20 µl with the sample and kit components. The reactions were performed using T100 Thermal Cycler (Bio-Rad). Finally, the cDNA samples were stored at -20 ºC until qRT-PCR measurements.

### 4.2.2 qRT-PCR measurements

The genes selected for closer investigation in the present study were chosen based on literature and with the help of CellMarker database (Zhang et al., 2019) in which the data concerning different biomarkers has been gathered comprehensively. The primary interest in the present study was in the genes involved in angiogenesis, but also to find

new housekeeping genes for turquoise killifish as control genes. Primer design for selected genes was performed with the help of NCBI primer design tool (Ye et al., 2012). The primers for angiogenesis-related genes *vcam1, tie1, cd34*, *vegfa,* melanoma cell adhesion molecule and lymphatic vessel endothelial hyaluronan receptor 1 were selected for the study. Housekeeping genes *tbp,* insulin receptor and hypoxanthine guanine phosphoribosyl transferase were tested for their potential as normalization genes. For each gene, the selected primers were evaluated for the specificity of the amplification signal (appendix 2).

Before qRT-PCR measurements the prepared cDNA samples were diluted to 1:10 with nuclease-free sterile water (Accugene) for obtaining the final RNA concentration of 0,5 or 1 ng/µl. For the amplification and detection in PCR reactions, SYBR Green PCR Master Mix (Applied Biosystems) was used. qRT-PCR measurements were performed using diluted cDNA samples, and four replicates for each sample were prepared. 8 µl of prepared master mix containing forward and reverse primers and 2 µl of diluted cDNA were pipetted into the wells of 96-well PCR plates to obtain 10 µl reaction volume per replicate. Sterile water was used as a negative control. The plates were sealed with adhesive seal, centrifuged in 2200g for 2 minutes, vortexed on a plate mixer and centrifuged again in 3500 rpm for 2 minutes. The run files with settings (appendix 3) were prepared using QuantStudio 12kFlex Real-Time PCR System software and the actual qRT-PCR measurements were performed by Plate Running Service at Turku Bioscience Center. The results were evaluated in relative quantification application by Thermo Fisher Cloud.

### 4.2.3 Tissue processing for histology

The regenerated pieces of caudal fins collected in March 2020 from turquoise killifish MZSC222 after drug study had been fixed and stored in 10 % neutral buffered formalin (FF-Chemicals) until September 2020. The fin pieces were further processed and embedded to paraffin on a frontal plane in histology service provider HistoCore, University of Turku, through an ascending series of ethanol (70 %, 96 % and absolute) and clearing in xylene. After processing, 4 µm sections from embedded samples were cut with a microtome in HistoCore. Prior to MG and PHH3 & CNA35 double staining, the paraffin was removed from the sections with xylene (Sigma-Aldrich) and the sections

were rehydrated through a descending series (absolute, 96 % and 70 %) of ethanol (VWR Chemicals).

### 4.2.4 Masson Goldner's staining

One section from each caudal fin sample embedded in paraffin was stained using MG staining kit for histology (Sigma-Aldrich) intended for visualizing connective tissue. Weigert's iron hematoxylin kit (Sigma-Aldrich) was used for nuclear staining. The staining was otherwise done according to the protocols of the kits, except for the incubation times for light green and hematoxylin. Due to the low color intensity, the incubation times were prolonged from 5 minutes to 12 minutes (light green) and from 2 minutes to 12 minutes (hematoxylin). The stained sections were mounted with Depex (Merck). After overnight drying at room temperature, the sections were scanned with Pannoramic P1000 Digital Slide Scanner (3D Histech). The scan files in mrxs file format were converted with 3D Histech converter for enabling the images to be opened in QuPath (version 0.2.3) software, a free platform for analyzing histological whole image slides (Bankhead et al., 2017). In QuPath, the number of blood vessels in each section was manually calculated. Analysis was done blinded.

### 4.2.5 Double staining of phospho-histone H3 and collagen-binding adhesion protein 35

PHH3 & CNA35 double staining was performed for 4 µm paraffin embedded fin sections. Polyclonal rabbit Phospho-Histone H3 (Ser10) Antibody (Cell Signaling) and Donkey anti-Rabbit secondary antibody conjugated with Alexa Fluor 647 (Invitrogen) were used for detecting mitotic cells in the tissue. CNA35 (Macherey-Nagel) fused into fluorescent pET28a mCherry vector was used for staining collagen. Purification of the protein had been done in 2019 by the technical assistants in the laboratory, and the purified probes were stored at -80°C until use. The protein concentration of the purified CNA35 mCherry was 7.65 mg/ml and molecular weight 60 kDa. The used concentrations were 1:200 (PHH3), 1:1000 (secondary antibody) and 1:100 (CNA35), and they were all diluted to 10 % FBS (Gibco) in PBS. After deparaffinization, antigen retrieval was performed in Retriever 2100 (Aptum Bio) using Universal Buffer (10x, R Universal, Aptum Bio) diluted to 1x concentration with MilliQ water. Following antigen retrieval, the two sections on each slide were circled with PAP pen (Invitrogen). Unspecific binding was

blocked by incubating sections in 10 % FBS for 1 hour. The slides were incubated with the primary antibody overnight at 4ºC protected from light. The other section on the slide was left as an unstained control, thus it was left without antibody. After overnight incubation, the primary antibody was washed away with PBS. Following PBS wash, the slides were incubated with secondary antibody at room temperature for 1 hour protected from light. For background staining, DAPI (Thermo Scientific) was diluted with PBS to the concentration of 0.002 mg/ml. Sections were incubated at room temperature for 10 minutes with DAPI protected from light. After washing with PBS, the slides were mounted with water based mounting media Mowiol 4-88 (Calbiochem) containing 2.5% DABCO (Sigma-Aldrich) as an antifading agent. The mounted slides were stored at 4°C protected from light. The mitotic cells and the collagen area in the sections were calculated and measured in Fiji image analysis software (Schindelin et al., 2012). Automatic thresholding was used for both analyses.

## 4.3 Wound healing study with young and old zebrafish

Wound healing studies with adult zebrafish were performed under the animal licenses ESAVI/16458/2019 and ESAVI/2402/2021 obtained from the Animal Experimental Board. 24 wild-type male zebrafish aged 4 months (12 fish) and 40 months (12 fish) were used for investigating wound healing between young and old zebrafish. At D0, the fish were individually anesthetized with tricaine methanosulfonate (Ethyl 3-aminobenzoate methanesulfonate, MS222, Sigma) diluted in system water to the concentration of 200 mg/l. As the depth of the anesthesia was deep enough, the fish was transferred on a petri dish lid. The caudal fin of the fish was carefully spread on top of the lid and photographed with a smart phone camera attached to Zeiss stereomicroscope. After this, a piece of caudal fin was cut away distally with a scalpel from the cleft in the center of the fin (figure 14 in Results) and the fin was photographed again. Finally, the fish was housed individually in a 1 l recovery tank containing 0.004 % of methylene blue in system water and placed in a warm room with the temperature of 26°C for the whole duration of the study. The tank water containing methylene blue was changed to fresh system water at 2 dpa and every other day after that. The caudal fin of the fish was photographed at D0, D2, D4, D6 and D8. The fish were fed every other day just before anaesthesia for photographing the caudal fin. At D8, the regenerated piece of caudal fin was cut away with a scalpel under anaesthesia and stored at -80°C. The fish used for the study were not

euthanized after the experiment but left alive for future mating purposes. The length of the regenerated part of the fin was measured manually in Fiji (Schindelin et al., 2012) both from the ventral and the dorsal side of the fin.

## 4.4 Drug study with larval zebrafish

According to EU Directive 2010/63/EU the use of zebrafish embryos/larvae for scientific purposes until the age of 5 dpf are not defined as protected, thus they are not subject to regulations concerning animal experiments. Therefore, no license for these experiments was needed. For each drug experiment, 3 male and 3 female fish from transgenic Casper zebrafish line *Tg(fli:EGFP)* were transferred to each 3 l mating tank filled with system water. The tanks were transferred overnight to a warm room with the temperature of 26°C and maintained at 12h light/12h dark cycle. Next morning the embryos were collected from mating tanks and checked under microscope for fertilization. The fertilized embryos were placed on ⌀10 cm petri dishes (approximately 50 eggs per dish) containing 25 ml of E3 incubation medium (0.33 mM $CaCl_2$, 0.33 mM $MgSO_4$, 5 mM NaCl and 0.17 mM KCl in MilliQ water). Finally, the petri dishes were transferred to incubator in the temperature of 28.5°C. The following day, at 1 dpf, the petri dishes were checked, and possible dead embryos were discarded. Embryos were also transferred to clean petri dishes containing fresh E3 medium. 20 µl of 20 mg/ml pronase E (*Streptomyces griseus* neutral proteinase, Actinase E; Serva) solution in E3 was also added for stimulating the hatching of the embryos.

At 2 dpf, the hatched embryos called larvae from 2 dpf onwards, were anesthetized in 0.16 g/l tricaine methanosulfonate (MS222, Sigma Aldrich) E3 solution containing 0.002 % Tween 20 (Sigma-Aldrich). The anesthetized larvae were placed on a petri dish with a small amount of tricaine solution. Approximately 1/3 of the total fin length measured from cloaca to the tip of the caudal fin was cut away distally with a scalpel (figure 18A in Results) under AxioZOOM V.16 microscope. Following the wounding, the larvae were also imaged under the microscope using Nikon 1x objective and 25x magnification. Finally, the larvae were transferred to a U-bottom 96-well plate and tricaine solution was carefully flushed away with E3 medium.

The test compounds for wound healing study were diluted to different concentrations (table 3) in DMSO (Sigma-Aldrich) or MilliQ water depending on the instructions in product specification sheets. Stock solutions from cobalt chloride, sodium nitroprusside, tazarotene and deferoxamine were prepared 2-5 days before the study and from semaxanib and roxadustat one year before the study. All the stocks were stored at -20ºC. Three concentrations for each compound were selected for this study based on literature (table 3). Prepared stocks were further diluted to E3 medium prior to the start of the treatment to obtain the chosen concentrations. Depending on the mating success, the larvae were randomly divided to groups of 12-20 larvae/concentration for the study. The treatment was started by replacing E3 medium in wells with 200 µl of test compound or control solution (E3 or 1 % DMSO in E3). The larvae were kept in the incubator at the temperature of 28.5°C for 48 hours and then anesthetized again by adding 10 µl of 4 g/l tricaine solution in each well of the 96-well plate. After this they were individually transferred on a petri dish and imaged under AxioZOOM V.16 microscope with the same settings as in the beginning of the study. Finally, the larvae within the same concentration of the compound in question were pooled and fixed overnight with 4 % paraformaldehyde (Thermo Fisher Scientific) in PBS containing 0.2 % of Tween 20 at 4°C. The length of the regenerated caudal fin was manually measured in in Fiji (Schindelin et al., 2012).

**Table 3.** The used compounds and concentrations with possible references in larval zebrafish wound healing study.

| Compound | Manufacturer | Stock and solvent | Concentrations | References |
|---|---|---|---|---|
| Cobalt chloride | Sigma-Aldrich | 1 M in MilliQ water | 1*, 5* and 10 mM† | * Wu et al., 2015<br>† Saeedi Saravi et al., 2009 |
| Deferoxamine | Sigma-Aldrich | 10 mM in MilliQ water | 1, 10†, and 100*† µM | * Pawar et al., 2020<br>† Chen et al., 2014 |
| Roxadustat | Cayman Chemical Company | 25 mM in DMSO | 2.5*, 15† and 50† µM | * Jain et al., 2016<br>† Kim et al., 2020 |
| Semaxanib | Santa Cruz Biotechnology Inc. | 10 mM in DMSO | 0.1, 1* and 10 µM | * Farooq et al., 2018 |
| Sodium nitroprusside | Sigma-Aldrich | 10 mM in MilliQ water | 0.1, 1* and 10 µM | * Leite at al., 2012 |
| Tazarotene | Sigma-Aldrich | 20 mM in DMSO | 1; 3* and 9 µM | * Al Haj Zen et al., 2016 |

## 4.5 Statistical methods

All statistical analyses were performed in GraphPad Prism version 9.0.0 for Mac (La Jolla, California, USA, www.graphpad.com). For histological and gene expression analyses, one-way ANOVA followed by Dunnett's post-hoc test for multiple comparisons was used for comparing the differences between the groups in the drug study. Two-way ANOVA followed by Šidák's multiple comparisons test was used for comparing the differences in caudal fin regeneration between old and young zebrafish. In addition, two-way ANOVA followed by Šidák's multiple comparisons test was used for the comparing the gene expression between young and middle-aged turquoise killifish. For investigating the statistical differences in the survival of two different turquoise killifish strains, a Log-rank test was performed. A $p$ value of $< 0.05$ was considered significant in all analyses, and NS indicates a $p$ value of $> 0.05$. One asterisk indicates a $p$ value from $< 0.05$ to 0.01, two asterisks a $p$ value from $< 0.01$ to 0.001, three asterisks a $p$ value from $< 0.001$ to 0.0001 and four asterisks a $p$ value of $< 0.0001$.

# 5. Acknowledgements

This thesis project was conducted at Turku Bioscience Center under the supervision of Ilkka Paatero. I would sincerely like to thank him for all the guidance, support and highly appreciated scientific discussion and comments throughout the thesis project. I would also like to thank the personnel in Johanna Ivaska's research group and in Zebrafish Core. It has been a pleasure to get to know people and be a part of this talented scientific community at Turku Bioscience Center. Finally, I would like to thank my family for being supportive during my master's studies.

# 6. Abbreviations list

| | |
|---|---|
| Ang-1 | angiopoietin 1 |
| CD34 | cluster of differentiation-34 |
| CNA35 | collagen-binding adhesion protein 35 |
| D | study day |
| dpa | day(s) post amputation |
| dpf | day(s) post fertilization |
| HIF-1α | hypoxia-inducible factor 1α |
| MG | Masson-Goldner's |
| MMP | matrix metalloproteinase |
| NO | nitric oxide |
| PHH3 | phospho-histone H3 |
| RAR | retinoid acid receptor |
| ROS | reactive oxygen species |
| Tbp | tata-box binding protein |
| Tie1 | receptor tyrosine kinase with immunoglobulin-like and EGF-like domains 1 |
| VCAM-1 | vascular adhesion molecule 1 |
| VEGFR | vascular endothelial growth factor receptor |

# 7. References


Acker, T., and K.H. Plate. 2003. Role of hypoxia in tumor angiogenesis—molecular and cellular angiogenic crosstalk. *Cell Tissue Res.* 314:145-155. doi: 10.1007/s00441-003-0763-8.

Adzick, N.S., and M.T. Longaker. 1992. Scarless fetal healing. Therapeutic implications. *Ann.Surg.* 215:3-7. doi: 10.1097/00000658-199201000-00004.

Agassandian, M., J.R. Tedrow, J. Sembrat, D.J. Kass, Y. Zhang, E.A. Goncharova, N. Kaminski, R.K. Mallampalli, and L.J. Vuga. 2015. VCAM-1 is a TGF-β1 inducible gene upregulated in idiopathic pulmonary fibrosis. *Cell.Signal.*27:2467-2473. doi: S0898-6568(15)00264-8.

Al Haj Zen, A., D.A. Nawrot, A. Howarth, A. Caporali, D. Ebner, A. Vernet, J.E. Schneider, and S. Bhattacharya. 2016. The Retinoid Agonist Tazarotene Promotes Angiogenesis and Wound Healing. *Molecular Therapy.* 24:1745-1759. doi: 10.1038/mt.2016.153.

Alderton, W.K., C.E. Cooper, and R.G. Knowles. 2001. Nitric oxide synthases: structure, function and inhibition. *Biochem.J.* 357:593-615. doi: 10.1042/0264-6021:3570593.

Aleström, P., L. D'Angelo, P.J. Midtlyng, D.F. Schorderet, S. Schulte-Merker, F. Sohm, and S. Warner. 2020. Zebrafish: Housing and husbandry recommendations. *Lab.Anim.* 54:213-224. doi: 10.1177/0023677219869037.

AnAge. 2021. The Animal Ageing and Longevity Database. AnAge entry for *Danio rerio*, https://genomics.senescence.info/species/entry.php?species=Danio_rerio (accessed May 4, 2021).

Anchelin, M., L. Murcia, F. Alcaraz-Pérez, E. García-Navarro M., and M.L. Cayuela. 2011. Behaviour of telomere and telomerase during aging and regeneration in zebrafish. *PloS One.* 6:e16955. doi: 10.1371/journal.pone.0016955.

Aper, S.J.A., A. van Spreeuwel C.C., M. van Turnhout C., A. van der Linden J., P.A. Pieters, N. van der Zon L.L., S. de la Rambelje L., C.V.C. Bouten, and M. Merkx. 2014. Colorful protein-based fluorescent probes for collagen imaging. *PloS One.* 9:e114983. doi: 10.1371/journal.pone.0114983.

Arcidiacono, B., E. Chiefari, A. Foryst-Ludwig, G. Currò, G. Navarra, F.S. Brunetti, M. Mirabelli, D.M. Corigliano, U. Kintscher, D. Britti, V. Mollace, D.P. Foti, I.D. Goldfine, and A. Brunetti. 2020. Obesity-related hypoxia via miR-128 decreases insulin-receptor expression in human and mouse adipose tissue promoting systemic insulin resistance. *EBioMedicine.* 59:102912. doi: 10.1016/j.ebiom.2020.102912.

Ashcroft, G.S., M.A. Horan, and M.W. Ferguson. 1998. Aging alters the inflammatory and endothelial cell adhesion molecule profiles during human cutaneous wound healing. *Lab.Invest.* 78:47-58.

Ashcroft, G.S., S.J. Mills, and J.J. Ashworth. 2002. Ageing and wound healing. *Biogerontology.* 3:337-345. doi: 5100237.

AstraZeneca. 2021. Further update on US regulatory review of roxadustat in anaemia of chronic kidney disease. Press release March 1, 2021. https://www.astrazeneca.com/media-centre/press-releases/2021/further-update-on-us-regulatory-review-of-roxadustat-in-anaemia-of-chronic-kidney-disease.html (accessed May 5, 2021).

Aurora, A.B., and E.N. Olson. 2014. Immune modulation of stem cells and regeneration. *Cell.Stem Cell.* 15:14-25. doi: S1934-5909(14)00257-4.

Azevedo, A.S., B. Grotek, A. Jacinto, G. Weidinger, and L. Saúde. 2011. The regenerative capacity of the zebrafish caudal fin is not affected by repeated amputations. *PLoS One.* 6:e22820. doi: 10.1371/journal.pone.0022820.

Azevedo, A.S., S. Sousa, A. Jacinto, and L. Saúde. 2012. An amputation resets positional information to a proximal identity in the regenerating zebrafish caudal fin. *BMC Developmental Biology.* 12:24. doi: 10.1186/1471-213X-12-24.

Bankhead, P., M.B. Loughrey, J.A. Fernández, Y. Dombrowski, D.G. McArt, P.D. Dunne, S. McQuaid, R.T. Gray, L.J. Murray, H.G. Coleman, J.A. James, M. Salto-Tellez, and P.W. Hamilton. 2017. QuPath: Open source software for digital pathology image analysis. *Scientific Reports.* 7:16878. doi: 10.1038/s41598-017-17204-5.

Bechter, R., G.D. Terlouw, M. Tsuchiya, T. Tsuchiya, and A. Kistler. 1992. Teratogenicity of arotinoids (retinoids) in the rat whole embryo culture. *Arch.Toxicol.* 66:193-197. doi: 10.1007/BF01974014.

Bentov, I., and M.J. Reed. 2014. Anesthesia, microcirculation, and wound repair in aging. *Anesthesiology.* 120:760-772. doi: 10.1097/ALN.0000000000000036.

Bernhardt, R.R., E. Tongiorgi, P. Anzini, and M. Schachner. 1996. Increased expression of specific recognition molecules by retinal ganglion cells and by optic pathway glia accompanies the successful regeneration of retinal axons in adult zebrafish. *J.Comp.Neurol.* 376:253-264. doi: 10.1002/(SICI)1096-9861(19961209)376:2<253::AID-CNE7>3.0.CO;2-2.

Besarab, A., R. Provenzano, J. Hertel, R. Zabaneh, S.J. Klaus, T. Lee, R. Leong, S. Hemmerich, K.P. Yu, and T.B. Neff. 2015. Randomized placebo-controlled dose-ranging and pharmacodynamics study of roxadustat (FG-4592) to treat anemia in nondialysis-dependent chronic kidney disease (NDD-CKD) patients. *Nephrology, Dialysis, Transplantation: Official Publication of the European Dialysis and Transplant Association - European Renal Association.* 30:1665-1673. doi: 10.1093/ndt/gfv302.

Blažek, R., M. Polačik, and M. Reichard. 2013a. Rapid growth, early maturation and short generation time in African annual fishes. *EvoDevo.* 4:24. doi: 10.1186/2041-9139-4-24.

Blum, N., and G. Begemann. 2012. Retinoic acid signaling controls the formation, proliferation and survival of the blastema during adult zebrafish fin regeneration. *Development.* 139:107-116. doi: 10.1242/dev.065391.

Bonham, C.A., M. Rodrigues, M. Galvez, A. Trotsyuk, Z. Stern-Buchbinder, M. Inayathullah, J. Rajadas, and G.C. Gurtner. 2018. Deferoxamine can prevent pressure ulcers and accelerate healing in aged mice. *Wound Rep and Reg.*26:300-305. doi: 10.1111/wrr.12667.

Bootle-Wilbraham, C.A., S. Tazzyman, W.D. Thompson, C.M. Stirk, and C.E. Lewis. 2001. Fibrin fragment E stimulates the proliferation, migration and differentiation of human microvascular endothelial cells in vitro. *Angiogenesis.*4:269-275. doi: 10.1023/a:1016076121918.

Bove, P.F., U.V. Wesley, A.K. Greul, M. Hristova, W.R. Dostmann, and A. van der Vliet. 2007. Nitric oxide promotes airway epithelial wound repair through enhanced activation of MMP-9. *Am.J.Respir.Cell Mol.Biol.* 36:138-146. doi: 2006-0253SM.

Bowers, S., and E. Franco. 2020. Chronic Wounds: Evaluation and Management. *Am.Fam.Physician.* 101:159-166. doi: 14456.

Brine Shrimp Direct. 2021. What are the guidelines for culturing brine shrimp? https://www.brineshrimpdirect.com/about-us/frequently-asked-questions/what-guidelines-culturing-brine-shrimp/ (accessed June 10, 2021).

Brown, N.J., E.A.E. Smyth, S.S. Cross, and M.W.R. Reed. 2002. Angiogenesis induction and regression in human surgical wounds. *Wound Repair and Regeneration.* 10:245-251. doi: 10.1046/j.1524-475X.2002.10408.x.

Burke, A.J., F.J. Sullivan, F.J. Giles, and S.A. Glynn. 2013. The yin and yang of nitric oxide in cancer progression. *Carcinogenesis.* 34:503-512. doi: 10.1093/carcin/bgt034.

Cancer Network. 2003. When New Drugs Fail: An Analysis of the SU5416 Trial Experience. *Oncology NEWS International*. 12:2. https://www.cancernetwork.com/view/when-new-drugs-fail-analysis-su5416-trial-experience (accessed August 20, 2021).

Cardeira, J., P.J. Gavaia, I. Fernández, I.F. Cengiz, J. Moreira-Silva, J.M. Oliveira, R.L. Reis, M.L. Cancela, and V. Laizé. 2016. Quantitative assessment of the regenerative and mineralogenic performances of the zebrafish caudal fin. *Scientific Reports.* 6:39191. doi: 10.1038/srep39191.

Carmeliet, P., and R.K. Jain. 2011. Molecular mechanisms and clinical applications of angiogenesis. *Nature.*473:298-307. doi: 10.1038/nature10144.

Carreiro, S., S. Anderson, H.J. Gukasyan, A. Krauss, and G. Prasanna. 2009. Correlation of In Vitro and In Vivo Kinetics of Nitric Oxide Donors in Ocular Tissues. *Journal of Ocular Pharmacology and Therapeutics.* 25:105-112. doi: 10.1089/jop.2008.0091.

Cellerino, A., D.R. Valenzano, and M. Reichard. 2016. From the bush to the bench: the annual Nothobranchius fishes as a new model system in biology. *Biological Reviews.* 91:511-533. doi: 10.1111/brv.12183.

Chang, E.I., S.A. Loh, D.J. Ceradini, E.I. Chang, S.E. Lin, N. Bastidas, S. Aarabi, D.A. Chan, M.L. Freedman, A.J. Giaccia, and G.C. Gurtner. 2007. Age decreases endothelial progenitor cell recruitment through decreases in hypoxia-inducible factor 1alpha stabilization during ischemia. *Circulation.* 116:2818-2829. doi: CIRCULATIONAHA.107.715847.

Chen, B., Y. Yan, C. Liu, L. Bo, G. Li, H. Wang, and Y. Xu. 2014. Therapeutic Effect of Deferoxamine on Iron Overload-Induced Inhibition of Osteogenesis in a Zebrafish Model. *Calcif.Tissue Int.* 94. doi: 10.1007/s00223-013-9817-4.

Chen, Q., X.H. Zhang, and J. Massagué. 2011. Macrophage binding to receptor VCAM-1 transmits survival signals in breast cancer cells that invade the lungs. *Cancer.Cell.* 20:538-549. doi: 10.1016/j.ccr.2011.08.025.

Childs, B.G., M. Durik, D.J. Baker, and J.M. van Deursen. 2015. Cellular senescence in aging and age-related disease: from mechanisms to therapy. *Nat.Med.* 21:1424-1435. doi: 10.1038/nm.4000.

Cho, Y., R. Sloutsky, K.M. Naegle, and V. Cavalli. 2013. Injury-induced HDAC5 nuclear export is essential for axon regeneration. *Cell.* 155:894-908. doi: S0092-8674(13)01277-4.

Collins, M.D. and G.E. Mao. 1999, Teratology of Retinoids. *Annu.Rev.Pharmacol.Toxicol*. 39:399-430. doi: 10.1146/annurev.pharmtox.39.1.399.

Conway, E.M., D. Collen, and P. Carmeliet. 2001. Molecular mechanisms of blood vessel growth. *Cardiovasc.Res.*49:507-521. doi: S0008636300002819.

Cook-Mills, J.M., M.E. Marchese, and H. Abdala-Valencia. 2011. Vascular cell adhesion molecule-1 expression and signaling during disease: regulation by reactive oxygen species and antioxidants. *Antioxid.Redox Signal.* 15:1607-1638. doi: 10.1089/ars.2010.3522.

D'Amico, G., E.A. Korhonen, A. Anisimov, G. Zarkada, T. Holopainen, R. Hägerling, F. Kiefer, L. Eklund, R. Sormunen, H. Elamaa, R.A. Brekken, R.H. Adams, G.Y. Koh, P. Saharinen, and K. Alitalo. 2014. Tie1 deletion inhibits tumor growth and improves angiopoietin antagonist therapy. *J.Clin.Invest.* 124:824-834. doi: 68897.

Dang, C.M., S.R. Beanes, H. Lee, X. Zhang, C. Soo, and K. Ting. 2003. Scarless fetal wounds are associated with an increased matrix metalloproteinase-to-tissue-derived inhibitor of metalloproteinase ratio. *Plast.Reconstr.Surg.*111:2273-2285. doi: 10.1097/01.PRS.0000060102.57809.DA.

Dang, M., R.E. Henderson, L.A. Garraway, and L.I. Zon. 2016. Long-term drug administration in the adult zebrafish using oral gavage for cancer preclinical studies. *Disease Models & Mechanisms.* 9:811-820. doi: 10.1242/dmm.024166.

Davies, D. 2003. Understanding biofilm resistance to antibacterial agents. *Nat.Rev.Drug Discov.* 2:114-122. doi: nrd1008.

Deeti, S., S. O'Farrell, and B.N. Kennedy. 2014. Early safety assessment of human oculotoxic drugs using the zebrafish visualmotor response. *J.Pharmacol.Toxicol.Methods*. 69:1-8. doi: 10.1016/j.vascn.2013.09.002.

Directive 2010/63/EU. 2010. European Union (EU) legislation on the protection of animals used for scientific purposes. https://eur-lex.europa.eu/LexUriServ/LexUriServ.do?uri=OJ:L:2010:276:0033:0079:en:PDF (accessed March 10, 2021).

Dodzian, J., S. Kean, J. Seidel, and D.R. Valenzano. 2018. A Protocol for Laboratory Housing of Turquoise Killifish (Nothobranchius furzeri). *J.Vis.Exp.* (134):57073. doi:10.3791/57073. doi: 10.3791/57073.

Dreßler, J., L. Bachmann, R. Koch, and E. Müller. 1999. Estimation of wound age and VCAM-1 in human skin. *Int.J.Legal Med.* 112:159-162. doi: 10.1007/s004140050223.

Dunnill, C., T. Patton, J. Brennan, J. Barrett, M. Dryden, J. Cooke, D. Leaper, & N. T. Georgopoulos. 2017. Reactive oxygen species (ROS) and wound healing: the functional role of ROS and emerging ROS-modulating technologies for augmentation of the healing process. *International wound journal*, 14(1), 89–96. doi: 10.1111/iwj.12557

Eming, S.A., T. Krieg, and J.M. Davidson. 2007. Inflammation in wound repair: molecular and cellular mechanisms. *J.Invest.Dermatol.* 127:514-525. doi: S0022-202X(15)33291-7.

Eming, S.A., P. Martin, and M. Tomic-Canic. 2014. Wound repair and regeneration: Mechanisms, signaling, and translation. *Science Translational Medicine.* 6:265sr6. doi: 10.1126/scitranslmed.3009337.

Eyries, M., G. Siegfried, M. Ciumas, K. Montagne, M. Agrapart, F. Lebrin, and F. Soubrier. 2008. Hypoxia-induced apelin expression regulates endothelial cell proliferation and regenerative angiogenesis. *Circ.Res.* 103:432-440. doi: 10.1161/CIRCRESAHA.108.179333.

Farooq, M., Z.M. Al Marhoon, N.A. Taha, A.A. Baabbad, M.A. Al-Wadaan, and A. El-Faham. 2018. Synthesis of Novel Class of N-Alkyl-isatin-3-iminobenzoic Acid Derivatives and Their Biological Activity in Zebrafish Embryos and Human Cancer Cell Lines. *Biol.Pharm.Bull.* 41:350-359. doi: 10.1248/bpb.b17-00674.

Fearnley, G.W., A.F. Odell, A.M. Latham, N.A. Mughal, A.F. Bruns, N.J. Burgoyne, S. Homer-Vanniasinkam, I.C. Zachary, M.C. Hollstein, S.B. Wheatcroft, and S. Ponnambalam. 2014. VEGF-A isoforms differentially regulate ATF-2-dependent VCAM-1 gene expression and endothelial-leukocyte interactions. *Mol.Biol.Cell.* 25:2509-2521. doi: 10.1091/mbc.E14-05-0962.

Ferrara, N. 2004. Vascular Endothelial Growth Factor: Basic Science and Clinical Progress. *Endocr.Rev.* 25:581-611. doi: 10.1210/er.2003-0027.

Field, F.K., and M.D. Kerstein. 1994. Overview of wound healing in a moist environment. *Am.J.Surg.* 167:2S-6S. doi: 0002-9610(94)90002-7.

FibroGen. 2018. FibroGen announces approval of roxadustat in China for the treatment of anemia in chronic kidney disease patients on dialysis. Press release17 Dec 2018. http://investor.fibrogen.com/phoenix.zhtml?c=253783&p=irol-newsArticle&ID=2380952 (accessed August 22, 2021).

Fong, T.A., L.K. Shawver, L. Sun, C. Tang, H. App, T.J. Powell, Y.H. Kim, R. Schreck, X. Wang, W. Risau, A. Ullrich, K.P. Hirth, and G. McMahon. 1999. SU5416 is a potent and selective inhibitor of the vascular endothelial growth factor receptor (Flk-1/KDR) that inhibits tyrosine kinase catalysis, tumor vascularization, and growth of multiple tumor types. *Cancer Res.* 59:99-106. https://cancerres.aacrjournals.org/content/canres/59/1/99.full.pdf (accessed August 23, 2021).

Frykberg, R.G., and J. Banks. 2015. Challenges in the Treatment of Chronic Wounds. *Advances in Wound Care.*4:560-582. doi: 10.1089/wound.2015.0635.

Genade, T., M. Benedetti, E. Terzibasi Tozzini, P. Roncaglia, D. Valenzano, A. Cattaneo, and A. Cellerino. 2005. Annual fishes of the genus Nothobranchius as a model system for aging research. *Aging Cell.* 4:223-33. doi: 10.1111/j.1474-9726.2005.00165.x.

Géraudie, J., M.J. Monnot, A. Brulfert, and P. Ferretti. 1995. Caudal fin regeneration in wild type and long-fin mutant zebrafish is affected by retinoic acid. *Int.J.Dev.Biol.* 39:373-381. doi: 10.1387/IJDB.7669548.

Gerhard, G.S., E.J. Kauffman, X. Wang, R. Stewart, J.L. Moore, C.J. Kasales, E. Demidenko, and K.C. Cheng. 2002. Life spans and senescent phenotypes in two strains of Zebrafish (Danio rerio). *Exp.Gerontol.* 37:1055-1068. doi: S0531556502000888.

Gerhardt, H., M. Golding, M. Fruttiger, C. Ruhrberg, A. Lundkvist, A. Abramsson, M. Jeltsch, C. Mitchell, K. Alitalo, D. Shima, and C. Betsholtz. 2003. VEGF guides angiogenic sprouting utilizing endothelial tip cell filopodia. *J.Cell Biol.*161:1163-1177. doi: 10.1083/jcb.200302047.

Gillitzer, R., and M. Goebeler. 2001. Chemokines in cutaneous wound healing. *J.Leukoc.Biol.* 69:513-521. doi: 10.1189/jlb.69.4.513.

Gonzalez, Ana Cristina de Oliveira, T.F. Costa, Z.d.A. Andrade, and Medrado, Alena Ribeiro Alves Peixoto. 2016. Wound healing - A literature review. *An.Bras.Dermatol.* 91:614-620. doi: 10.1590/abd1806-4841.20164741.

González-Rosa, J.M., G. Guzmán-Martínez, I.J. Marques, H. Sánchez-Iranzo, L.J. Jiménez-Borreguero, and N. Mercader. 2014. Use of Echocardiography Reveals Reestablishment of Ventricular Pumping Efficiency and Partial Ventricular Wall Motion Recovery upon Ventricular Cryoinjury in the Zebrafish. *Plos One.* 9:e115604.

Górnikiewicz, B., A. Ronowicz, J. Podolak, P. Madanecki, A. Stanisławska-Sachadyn, and P. Sachadyn. 2013. Epigenetic basis of regeneration: analysis of genomic DNA methylation profiles in the MRL/MpJ mouse. *DNA Res.* 20:605-621. doi: 10.1093/dnares/dst034.

Grunewald, M., S. Kumar, H. Sharife, E. Volinsky, A. Gileles-Hillel, T. Licht, A. Permyakova, L. Hinden, S. Azar, Y. Friedmann, P. Kupetz, R. Tzuberi, A. Anisimov, K. Alitalo, M. Horwitz, S. Leebhoff, O.Z. Khoma, R. Hlushchuk, V. Djonov, R. Abramovitch, J. Tam, and E. Keshet. 2021. Counteracting age-related VEGF signaling insufficiency promotes healthy aging and extends life span. *Science.* 373:eabc8479. doi: 10.1126/science.abc8479.

Hamilton, J.L., A. Hatef, M. Imran ul-haq, N. Nair, S. Unniappan, and J.N. Kizhakkedathu. 2014. Clinically Approved Iron Chelators Influence Zebrafish Mortality, Hatching Morphology and Cardiac Function. *Plos One.* doi: 10.1371/journal.pone.0109880.

Han, E., K. Ho Oh, S. Park, Y. Chan Rah, H. Park, S. Koun, and J. Choi. 2020. Analysis of behavioral changes in zebrafish (Danio rerio) larvae caused by aminoglycoside-induced damage to the lateral line and muscles. *Neurotoxicology.* 78:134-142. doi: 10.1016/j.neuro.2020.03.005.

Hanahan, D., and J. Folkman. 1996. Patterns and Emerging Mechanisms of the Angiogenic Switch during Tumorigenesis. *Cell.* 86:353-364. doi: 10.1016/S0092-8674(00)80108-7.

Hans, F., and S. Dimitrov. 2001. Histone H3 phosphorylation and cell division. *Oncogene.* 20:3021-3027. doi: 10.1038/sj.onc.1204326.

Haroon, Z., K. Amin, W. Saito, W. Wilson, C. Greenberg, and M. Dewhirst. 2002. SU5416 Delays Wound Healing Through Inhibition of TGF-β Activation. *Cancer Biology & Therapy.* 1:121-6. doi: 10.4161/cbt.55.

Hartmann, N., K. Reichwald, A. Lechel, M. Graf, J. Kirschner, A. Dorn, E. Terzibasi, J. Wellner, M. Platzer, K.L. Rudolph, A. Cellerino, and C. Englert. 2009. Telomeres shorten while Tert expression increases during ageing of the short-lived fish Nothobranchius furzeri. *Mech.Ageing Dev.* 130:290-296. doi: 10.1016/j.mad.2009.01.003.

Hartmann, N., K. Reichwald, I. Wittig, S. Dröse, S. Schmeisser, C. Lück, C. Hahn, M. Graf, U. Gausmann, E. Terzibasi, A. Cellerino, M. Ristow, U. Brandt, M. Platzer, and C. Englert. 2011. Mitochondrial DNA copy number and function decrease with age in the short-lived fish Nothobranchius furzeri. *Aging Cell.* 10:824-831. doi: 10.1111/j.1474-9726.2011.00723.x.

Hedge, J., E. Sanders, K. Jarema, D. Hunter, and S. Padilla. 2017. Effect of Methylene Blue on Developing Zebrafish Embryos (Danio Rerio). Aquaculture America 2017, San Antonio, TX, February 19 - 22, 2017.

Hellberg, C., A. Ostman, and C.H. Heldin. 2010. PDGF and vessel maturation. *Recent Results Cancer Res.* 180:103-114. doi: 10.1007/978-3-540-78281-0_7.

Holden, P., and L.S. Nair. 2019. Deferoxamine: An Angiogenic and Antioxidant Molecule for Tissue Regeneration. *Tissue Eng.Part B.Rev.* 25:461-470. doi: 10.1089/ten.TEB.2019.0111.

Holme, M.R., and Sharman, T. 2020. Sodium Nitroprusside. *In* StatPearls. Treasure Island (FL): StatPearls Publishing. https://www.ncbi.nlm.nih.gov/books/NBK557487/ (accessed June 1, 2021).

Honnegowda, T.M., P. Kumar, E.G. Udupa, S. Kumar, U. Kumar, and P. Rao. 2015. Role of angiogenesis and angiogenic factors in acute and chronic wound healing. *Plast Aesthet Res.* 2:239-42. doi: 10.4103/2347-9264.165438.

Hou, Z., C. Nie, Z. Si, and Y. Ma. 2013. Deferoxamine enhances neovascularization and accelerates wound healing in diabetic rats via the accumulation of hypoxia-inducible factor-1α. *Diabetes Res.Clin.Pract.* 101:62-71. doi: 10.1016/j.diabres.2013.04.012.

Huang, J., J. Zhang, H. Li, Z. Lu, W. Shan, I. Mercado-Uribe, and J. Liu. 2013. VCAM1 expression correlated with tumorigenesis and poor prognosis in high grade serous ovarian cancer. *Am.J.Transl.Res.* 5:336-346.

Iovine, M.K. 2007. Conserved mechanisms regulate outgrowth in zebrafish fins. *Nat.Chem.Biol.* 3:613-618. doi: nchembio.2007.36.

Itou, J., H. Kawakami, T. Burgoyne, and Y. Kawakami. 2012. Life-Long Preservation of the Regenerative Capacity in the Fin and Heart in Zebrafish. *Biol. Open*. 1:739-746. doi:10.1242/bio.20121057.

Jaakkola, P., D.R. Mole, Y. Tian, M.I. Wilson, J. Gielbert, S.J. Gaskell, A.v. Kriegsheim, H.F. Hebestreit, M. Mukherji, C.J. Schofield, P.H. Maxwell, C.W. Pugh, and P.J. Ratcliffe. 2001. Targeting of HIF-α to the von Hippel-Lindau Ubiquitylation Complex by $O_2$-Regulated Prolyl Hydroxylation. *Science.* 292:468-472. doi: 10.1126/science.1059796.

Jain, I.H., L. Zazzeron, R. Goli, K. Alexa, S. Schatzman-Bone, H. Dhillon, O. Goldberger, J. Peng, O. Shalem, N.E. Sanjana, F. Zhang, W. Goessling, W.M. Zapol, and V.K. Mootha. 2016. Hypoxia as a therapy for mitochondrial disease. *Science.* 352(6281):54-61. doi: 10.1126/science.aad9642.

Johnson, K.E., and T.A. Wilgus. 2014. Vascular Endothelial Growth Factor and Angiogenesis in the Regulation of Cutaneous Wound Repair. *Adv.Wound.Care.(New Rochelle).* 3:647-661. doi: 10.1089/wound.2013.0517.

Jopling, C., S. Boue, and J.C. Izpisua Belmonte. 2011. Dedifferentiation, transdifferentiation and reprogramming: three routes to regeneration. *Nat.Rev.Mol.Cell Biol.* 12:79-89. doi: 10.1038/nrm3043.

Jubb, R. A. 1971. A new Nothobranchius (Pisces, Cyprinodontidae) from southeastern Rhodesia. *Journal of the American Killifish Association*. 8 (1): 12–19.

Kalan, L.R., J.S. Meisel, M.A. Loesche, J. Horwinski, I. Soaita, X. Chen, A. Uberoi, S.E. Gardner, and E.A. Grice. 2019. Strain- and Species-Level Variation in the Microbiome of Diabetic Wounds Is Associated with Clinical Outcomes and Therapeutic Efficacy. *Cell Host & Microbe.* 25:641-655.e5. doi: 10.1016/j.chom.2019.03.006.

Kazemi-Lomedasht, F., M. Behdani, K.P. Bagheri, M. Habibi-Anbouhi, M. Abolhassani, R. Arezumand, D. Shahbazzadeh, and H. Mirzahoseini. 2015. Inhibition of angiogenesis in human endothelial cell using VEGF specific nanobody. *Mol.Immunol.* 65:58-67. doi: S0161-5890(15)00012-7.

Kim, H.R., K. Santhakumar, E. Markham, D. Baldera, D. Greenald, H.E. Bryant, S.F. El-Khamisy, and F.J. van Eeden. 2020. Investigation of the role of VHL-HIF signaling in DNA repair and apoptosis in zebrafish. *Oncotarget.* 11:1109-1130. doi: 10.18632/oncotarget.27521.

Kim, I., S.O. Moon, S.H. Kim, H.J. Kim, Y.S. Koh, and G.Y. Koh. 2001. Vascular endothelial growth factor expression of intercellular adhesion molecule 1 (ICAM-1), vascular cell adhesion molecule 1 (VCAM-1), and E-selectin through nuclear factor-kappa B activation in endothelial cells. *J.Biol.Chem.* 276:7614-7620. doi: S0021-9258(19)67220-0.

Kishi, S., P.E. Bayliss, J. Uchiyama, E. Koshimizu, J. Qi, P. Nanjappa, S. Imamura, A. Islam, D. Neuberg, A. Amsterdam, and T.M. Roberts. 2008. The identification of zebrafish mutants showing alterations in senescence-associated biomarkers. *PLoS Genet.* 4(8):e1000152. doi: 10.1371/journal.pgen.1000152.

Kistler, A., T. Tsuchiya, M. Tsuchiya, and M. Klaus. 1990. Teratogenicity of arotinoids (retinoids) in vivo and in vitro. *Arch.Toxicol.* 64:616-622. doi: 10.1007/BF01974689.

Kiwanuka, E., J. Junker, and E. Eriksson. 2012. Harnessing growth factors to influence wound healing. *Clin.Plast.Surg.* 39:239-248. doi: 10.1016/j.cps.2012.04.003.

Knopf, F., C. Hammond, A. Chekuru, T. Kurth, S. Hans, C.W. Weber, G. Mahatma, S. Fisher, M. Brand, S. Schulte-Merker, and G. Weidinger. 2011. Bone regenerates via dedifferentiation of osteoblasts in the zebrafish fin. *Dev.Cell.*20:713-724. doi: 10.1016/j.devcel.2011.04.014.

Korhonen, J., J. Partanen, E. Armstrong, A. Vaahtokari, K. Elenius, M. Jalkanen, and K. Alitalo. 1992. Enhanced expression of the tie receptor tyrosine kinase in endothelial cells during neovascularization. *Blood.* 80:2548-2555. doi: S0006-4971(20)76664-4.

Kosonen, K. 2020. Mechanisms of aging induced decline in wound healing. Master's thesis. University of Turku. https://www.utupub.fi/handle/10024/150742 (accessed October 10, 2020).

Krug, J. 2021. Generating a transparent vertebrate model for in vivo applications in aging research. Online presentation at 4th Nothobranchius symposium.

Kumar, I., C.A. Staton, S.S. Cross, M.W. Reed, and N.J. Brown. 2009. Angiogenesis, vascular endothelial growth factor and its receptors in human surgical wounds. *Br.J.Surg.* 96:1484-1491. doi: 10.1002/bjs.6778.

Kyritsis, N., C. Kizil, and M. Brand. 2014. Neuroinflammation and central nervous system regeneration in vertebrates. *Trends Cell Biol.* 24:128-135. doi: S0962-8924(13)00137-2.

Lebrun, E., and R.S. Kirsner. 2013. Frequent debridement for healing of chronic wounds. *JAMA Dermatol.* 149:1059. doi: 10.1001/jamadermatol.2013.4959.

LeClair, E.E., and J. Topczewski. 2010. Development and Regeneration of the Zebrafish Maxillary Barbel: A Novel Study System for Vertebrate Tissue Growth and Repair. *Plos One.* 5(1):e8737. doi: 10.1371/journal.pone.0008737.

Leggieri, A., C. Attanasio, A. Palladino, A. Cellerino, C. Lucini, M. Paolucci, E. Terzibasi Tozzini, P. de Girolamo, and L. D'Angelo. 2019. Identification and Expression of Neurotrophin-6 in the Brain of Nothobranchius furzeri: One More Piece in Neurotrophin Research. *Journal of Clinical Medicine.* 8:595. doi: 10.3390/jcm8050595.

Leite, C.E., A. da Cruz Teixeira, F.F. Cruz, S.C. Concatto, J.H. Amaral, C.D. Bonan, M.M. Campos, F.B. Morrone, and A.M.O. Battastini. 2012. Analytical method for determination of nitric oxide in zebrafish larvae: Toxicological and pharmacological applications. *Anal.Biochem.* 421:534-540. doi: 10.1016/j.ab.2011.11.038.

Leonardi, R., M. Caltabiano, M. Pagano, V. Pezzuto, C. Loreto, and G. Palestro. 2003. Detection of Vascular Endothelial Growth Factor/Vascular Permeability Factor in Periapical Lesions. *J.Endod.* 29:180-183. doi: 10.1097/00004770-200303000-00004.

Li, J.J., Y.Q. Huang, R. Basch, and S. Karpatkin. 2001. Thrombin induces the release of angiopoietin-1 from platelets. *Thromb.Haemost.* 85:204-206. doi: 01020204.

Liang, Y., C. Liu, M. Lu, Q. Dong, Z. Wang, Z. Wang, W. Xiong, N. Zhang, J. Zhou, Q. Liu, X. Wang, and Z. Wang. 2018. Calorie restriction is the most reasonable anti-ageing intervention: a meta-analysis of survival curves. *Scientific Reports.* 8:5779. doi: 10.1038/s41598-018-24146-z.

Lindholm, C., and R. Searle. 2016. Wound management for the 21st century: combining effectiveness and efficiency. *Int Wound J.* 13:5-15. doi: 10.1111/iwj.12623.

Liu, P., X. Yang, J. Han, M. Zhao, J. Guo, R. Si, Z. Zhang, A. Wang, and J. Zhang. 2020. Tazarotene-loaded PLGA nanoparticles potentiate deep tissue pressure injury healing via VEGF-Notch signaling. *Materials Science and Engineering: C.* 114:111027. doi: 10.1016/j.msec.2020.111027.

Lo, B.C., M.J. Gold, S. Scheer, M.R. Hughes, J. Cait, E. Debruin, F.S.F. Chu, D.C. Walker, H. Soliman, F.M. Rossi, M. Blanchet, G. Perona-Wright, C. Zaph, and K.M. McNagny. 2017. Loss of vascular CD34 results in increased sensitivity to lung injury. *Am J Resp Cell Mol.* 57:651-661. doi: 10.1165/rcmb.2016-0386OC.

Mace, K., D. Yu, K. Paydar, N. Boudreau, and D. Young. 2007. Sustained expression of Hif-1 alpha in the diabetic environment promotes angiogenesis and cutaneous wound repair. *Wound Repair and Regeneration: Official Publication of the Wound Healing Society and] the European Tissue Repair Society.* 15:636-45. doi: 10.1111/j.1524-475X.2007.00278.x.

Maines, M.D., and P. Sinclair. 1977. Cobalt regulation of heme synthesis and degradation in avian embryo liver cell culture. *J.Biol.Chem.* 252:219-223. doi: S0021-9258(17)32819-3.

Malek, R.L., H. Sajadi, J. Abraham, M.A. Grundy, and G.S. Gerhard. 2004. The effects of temperature reduction on gene expression and oxidative stress in skeletal muscle from adult zebrafish. *Comp.Biochem.Physiol.C.Toxicol.Pharmacol.* 138:363-373. doi: S1532-0456(04)00151-6.

Marin, V., F.A. Montero-Julian, S. Grès, V. Boulay, P. Bongrand, C. Farnarier, and G. Kaplanski. 2001. The IL-6-soluble IL-6Ralpha autocrine loop of endothelial activation as an intermediate between acute and chronic inflammation: an experimental model involving thrombin. *J.Immunol.* 167:3435-3442. doi: 10.4049/jimmunol.167.6.3435.

Marques, I.J., E. Lupi, and N. Mercader. 2019. Model systems for regeneration: zebrafish. *Development.*146:dev167692. doi: 10.1242/dev.167692.

Martin, P. 1997. Wound healing--aiming for perfect skin regeneration. *Science.* 276:75-81. doi: 10.1126/science.276.5309.75.

Martins-Green, M., M. Petreaca, and L. Wang. 2013. Chemokines and Their Receptors Are Key Players in the Orchestra That Regulates Wound Healing. *Adv.Wound.Care.(New Rochelle).* 2:327-347. doi: 10.1089/wound.2012.0380.

Mathus-Vliegen, E.M. 2004. Old age, malnutrition, and pressure sores: an ill-fated alliance. *J.Gerontol.A Biol.Sci.Med.Sci.* 59:355-360. doi: 10.1093/gerona/59.4.m355.

McCarthy, M.J., M. Crowther, P. R.F. Bell, and N.P.J. Brindle. 1998. The endothelial receptor tyrosine kinase tie-1 is upregulated by hypoxia and vascular endothelial growth factor. *FEBS Lett.* 423:334-338. doi: 10.1016/S0014-5793(98)00122-7.

McCarty, S.M., and S.L. Percival. 2013. Proteases and Delayed Wound Healing. *Adv.Wound.Care.(New Rochelle).*2:438-447. doi: 10.1089/wound.2012.0370.

Mescher, A.L., and A.W. Neff. 2005. Regenerative capacity and the developing immune system. *Adv.Biochem.Eng.Biotechnol.* 93:39-66. doi: 10.1007/b99966.

Miao, M., B. Yuan, R. Mani, and S. Lu. 2013. Macrophage activation dysfunction in impaired wound healing: a potential therapeutic target. *Int.J.Low Extrem Wounds.* 12:239-241. doi: 10.1177/1534734613502052.

Misof, B.Y., and G.P. Wagner. 1992. Regeneration in Salaria pavo (Blenniidae, Teleostei). Histogenesis of the regenerating pectoral fin suggests different mechanisms for morphogenesis and structural maintenance. *Anat.Embryol.(Berl).* 186:153-165. doi: 10.1007/BF00174953.

Mogford, J.E., N. Tawil, A. Chen, D. Gies, Y. Xia, and T.A. Mustoe. 2002. Effect of age and hypoxia on TGFbeta1 receptor expression and signal transduction in human dermal fibroblasts: impact on cell migration. *J.Cell.Physiol.*190:259-265. doi: 10.1002/jcp.10060.

Muñoz-Sánchez, J., and M.E. Chánez-Cárdenas. 2019. The use of cobalt chloride as a chemical hypoxia model. *J.Appl.Toxicol.* 39:556-570. doi: 10.1002/jat.3749.

Nakayama, J., and H. Makinoshima. 2020. Zebrafish-Based Screening Models for the Identification of Anti-Metastatic Drugs. *Molecules.* 25:2407. doi:10.3390/molecules25102407.

Nasiadka, A., and M.D. Clark. 2012. Zebrafish Breeding in the Laboratory Environment. *Ilar J.* 53:161-168. doi: 10.1093/ilar.53.2.161.

Nathan, C. 2006. Neutrophils and immunity: challenges and opportunities. *Nat.Rev.Immunol.* 6:173-182. doi: nri1785.

National Center for Biotechnology Information. 2021a. PubChem Compound Summary for CID 2973, Deferoxamine. https://pubchem.ncbi.nlm.nih.gov/compound/Deferoxamine (accessed August 24, 2021).

National Center for Biotechnology Information. 2021b. PubChem Compound Summary for CID 5381, Tazarotene. https://pubchem.ncbi.nlm.nih.gov/compound/Tazarotene (accessed August 23, 2021).

Nechiporuk, A., and M.T. Keating. 2002. A proliferation gradient between proximal and msxb-expressing distal blastema directs zebrafish fin regeneration. *Development.* 129:2607-2617. doi: 10.1242/dev.129.11.2607.

Nguyen, M., J. Arkell, and C.J. Jackson. 2001. Human endothelial gelatinases and angiogenesis. *Int.J.Biochem.Cell Biol.* 33:960-970. doi: S1357-2725(01)00007-3.

Novak, M.L., and T.J. Koh. 2013. Phenotypic transitions of macrophages orchestrate tissue repair. *Am.J.Pathol.*183:1352-1363. doi: S0002-9440(13)00619-6.

Occleston, N.L., S. O'Kane, N. Goldspink, and M.W. Ferguson. 2008. New therapeutics for the prevention and reduction of scarring. *Drug Discov.Today.* 13:973-981. doi: 10.1016/j.drudis.2008.08.009.

Okur, M.E., I.D. Karantas, Z. Şenyiğit, N. Üstündağ Okur, and P.I. Siafaka. 2020. Recent trends on wound management: New therapeutic choices based on polymeric carriers. *Asian Journal of Pharmaceutical Sciences.* 15:661-684. doi: 10.1016/j.ajps.2019.11.008.

Owens, K.N., A.B. Coffin, L.S. Hong, K.O. Bennett, E.W. Rubel, and D.W. Raible. 2009. Response of mechanosensory hair cells of the zebrafish lateral line to aminoglycosides reveals distinct cell death pathways. *Hear.Res.* 253:32-41. doi: 10.1016/j.heares.2009.03.001.

Pan, T., Z. Wei, Y. Fang, Z. Dong, and W. Fu. 2018. Therapeutic efficacy of CD34+ cell-involved mononuclear cell therapy for no-option critical limb ischemia: A meta-analysis of randomized controlled clinical trials. *Vasc Med.* 23(3):219-231. doi: 10.1177/1358863X17752556.

Panetta, N.J., S. Ouyang, N. Quarto, J.K. Chen, and M.T. Longaker. 2008. Zebrafish maintain regenerative capacity with age. *J.Am.Coll.Surg.* 207:S65. doi: 10.1016/j.jamcollsurg.2008.06.161.

Pawar, N.V., P.D. Singh, P.S. Prabhu, and J.R. Rana. 2021. Carcinogen-Induced Model of Proangiogenesis in Zebrafish Embryo-Larvae. *Environ.Toxicol.Chem.* 40:447-453. doi: 10.1002/etc.4928.

Pelster, B., S. Grillitsch, and T. Schwerte. 2005. NO as a mediator during the early development of the cardiovascular system in the zebrafish. *Comparative Biochemistry and Physiology Part A: Molecular & Integrative Physiology.*142:215-220. doi: 10.1016/j.cbpb.2005.05.036.

Pfefferli, C., and A. Jaźwińska. 2015. The art of fin regeneration in zebrafish. *Regeneration (Oxf).* 2:72-83. doi: 10.1002/reg2.33.

Pfefferli, C., F. Müller, A. Jaźwińska, and C. Wicky. 2014. Specific NuRD components are required for fin regeneration in zebrafish. *BMC Biology.* 12:30. doi: 10.1186/1741-7007-12-30.

Phillips, C.J., I. Humphreys, J. Fletcher, K. Harding, G. Chamberlain, and S. Macey. 2016. Estimating the costs associated with the management of patients with chronic wounds using linked routine data. *Int Wound J.* 13:1193-1197. doi: 10.1111/iwj.12443.

Platzer, M., and C. Englert. 2016. Nothobranchius furzeri: A Model for Aging Research and More. *Trends in Genetics.*32:543-552. doi: 10.1016/j.tig.2016.06.006.

Posnett, J., and P.J. Franks. 2008. The burden of chronic wounds in the UK. *Nurs.Times.* 104:44-45. https://www.nursingtimes.net/clinical-archive/tissue-viability/the-burden-of-chronic-wounds-in-the-uk-23-01-2008/ (accessed May 20, 2021).

Polačik, M., R. Blažek, and M. Reichard. 2016. Laboratory breeding of the short-lived annual killifish Nothobranchius furzeri. *Nat.Protoc.* 11:1396-1413. doi: 10.1038/nprot.2016.080.

Poss, K.D., L.G. Wilson, and M.T. Keating. 2002. Heart Regeneration in Zebrafish. *Science.* 298:2188-2190. doi: 10.1126/science.1077857.

Product information sheet. 2021. Deferoxamine. Sigma. https://www.sigmaaldrich.com/deepweb/assets/sigmaaldrich/product/documents/387/917/d9533pis.pdf (accessed June 1, 2021).

Qi, L., A.R. Ahmadi, J. Huang, M. Chen, B. Pan, H. Kuwabara, K. Iwasaki, W. Wang, R. Wesson, A.M. Cameron, S. Cui, J. Burdick, and Z. Sun. 2020. Major Improvement in Wound Healing Through Pharmacologic Mobilization of Stem Cells in Severely Diabetic Rats. *Diabetes.* 69:699-712. doi: 10.2337/db19-0907.

Rajendran, N.K., S.S.D. Kumar, N.N. Houreld, and H. Abrahamse. 2018. A review on nanoparticle based treatment for wound healing. *Journal of Drug Delivery Science and Technology.* 44:421-430. doi: 10.1016/j.jddst.2018.01.009.

Ramachandran, P., and M. Thangavelu. 1969. A comparative study of wound healing. *Indian.J.Exp.Biol.* 7:148-151.

Reinke, J.M., and H. Sorg. 2012. Wound repair and regeneration. *Eur.Surg.Res.* 49:35-43. doi: 10.1159/000339613.

Rice, G.E., and M.P. Bevilacqua. 1989. An inducible endothelial cell surface glycoprotein mediates melanoma adhesion. *Science.* 246:1303-1306. doi: 10.1126/science.2588007.

Roberts, H.R., and A.H. Tabares. 1995. Overview of the coagulation reactions. *In* High KA, Roberts HR, editors. Molecular basis of thrombosis and hemostasis. New York: Marcel Dekker. pp. 35-50.

Rodrigues, M., N. Kosaric, C.A. Bonham, and G.C. Gurtner. 2019. Wound Healing: A Cellular Perspective. *Physiol.Rev.*99:665-706. doi: 10.1152/physrev.00067.2017.

Rowlatt, U. 1979. Intrauterine wound healing in a 20 week human fetus. *Virchows Arch.A Pathol.Anat.Histol.*381:353-361. doi: 10.1007/BF00432477.

Saeedi Saravi, S.S., S. Karami, B. Karami, and M. Shokrzadeh. 2009. Toxic effects of cobalt chloride on hematological factors of common carp (Cyprinus carpio). *Biol.Trace Elem.Res.* 132:144-152. doi: 10.1007/s12011-009-8388-8.

Sagayaraj, V., and R. Malathi. 2017. Impact of Hypoxia Induced VEGF and its Signaling during Caudal Fin Regeneration in Zebrafish. *bioRxiv*. doi: 10.1101/105767.

Sakao, S., and K. Tatsumi. 2011. The effects of antiangiogenic compound SU5416 in a rat model of pulmonary arterial hypertension. *Respiration.* 81:253-261. doi: 10.1159/000322011.

Santos-Ruiz, L., J.A. Santamaría, J. Ruiz-Sánchez, and J. Becerra. 2002. Cell proliferation during blastema formation in the regenerating teleost fin. *Dev.Dyn.* 223:262-272. doi: 10.1002/dvdy.10055.

Sargen, M.R., O. Hoffstad, and D.J. Margolis. 2013. Geographic variation in Medicare spending and mortality for diabetic patients with foot ulcers and amputations. *J.Diabetes Complications.* 27:128-133. doi: 10.1016/j.jdiacomp.2012.09.003.

Savant, S., S. La Porta, A. Budnik, K. Busch, J. Hu, N. Tisch, C. Korn, A.F. Valls, A.V. Benest, D. Terhardt, X. Qu, R.H. Adams, H.S. Baldwin, C. Ruiz de Almodóvar, H.R. Rodewald, and H.G. Augustin. 2015. The Orphan Receptor Tie1 Controls Angiogenesis and Vascular Remodeling by Differentially Regulating Tie2 in Tip and Stalk Cells. Cell.Rep. 12:1761-1773. doi: S2211-1247(15)00895-5.

Schindelin, J., I. Arganda-Carreras, E. Frise, V. Kaynig, M. Longair, T. Pietzsch, S. Preibisch, C. Rueden, S. Saalfeld, B. Schmid, J. Tinevez, D.J. White, V. Hartenstein, K. Eliceiri, P. Tomancak, and A. Cardona. 2012. Fiji: an open-source platform for biological-image analysis. *Nature Methods.* 9:676-682. doi: 10.1038/nmeth.2019.

Schreml, S., R.M. Szeimies, L. Prantl, S. Karrer, M. Landthaler, and P. Babilas. 2010. Oxygen in acute and chronic wound healing. *Br.J.Dermatol.* 163:257-268. doi: 10.1111/j.1365-2133.2010.09804.x.

Schultz, G.S., R.G. Sibbald, V. Falanga, E.A. Ayello, C. Dowsett, K. Harding, M. Romanelli, M.C. Stacey, L. Teot, and W. Vanscheidt. 2003. Wound bed preparation: a systematic approach to wound management. *Wound Repair Regen.* 11 Suppl 1:1. doi: 1129.

Sen, C.K., and Roy, S. 2012.Wound healing. *In* Rodriguez E, Losee J, Neligan PC, editors. Plastic Surgery: Volume 3: Craniofacial, Head and Neck Surgery and Pediatric Plastic Surgery. 3rd ed. Philadelphia: Saunders. pp. 240-66.

Sgonc, R., and J. Gruber. 2013. Age-Related Aspects of Cutaneous Wound Healing: A Mini-Review. *Gerontology.*59:159-164. doi: 10.1159/000342344.

Shao, J., D. Chen, Q. Ye, J. Cui, Y. Li, and L. Li. 2011. Tissue regeneration after injury in adult zebrafish: The regenerative potential of the caudal fin. *Dev.Dyn.* 240:1271-1277. doi: 10.1002/dvdy.22603.

Siemerink, M.J., I. Klaassen, I.M.C. Vogels, A.W. Griffioen, C. Van Noorden J.F., and R.O. Schlingemann. 2012. CD34 marks angiogenic tip cells in human vascular endothelial cell cultures. *Angiogenesis.* 15:151-163. doi: 10.1007/s10456-011-9251-z.

Singer, A.J., and R.A. Clark. 1999. Cutaneous wound healing. *N.Engl.J.Med.* 341:738-746. doi: 10.1056/NEJM199909023411006.

Smith, R.S., L. Gao, G. Bledsoe, L. Chao, and J. Chao. 2009. Intermedin is a new angiogenic growth factor. *American Journal of Physiology-Heart and Circulatory Physiology.* 297:H1040-H1047. doi: 10.1152/ajpheart.00404.2009.

Stevens, L.J., and A. Page-McCaw. 2012. A secreted MMP is required for reepithelialization during wound healing. *Mol.Biol.Cell.* 23:1068-1079. doi: 10.1091/mbc.E11-09-0745.

Tang, D., J. Zhang, T. Yan, J. Wei, X. Jiang, D. Zhang, Q. Zhang, J. Jia, and Y. Huang. 2018. FG-4592 Accelerates Cutaneous Wound Healing by Epidermal Stem Cell Activation via HIF-1α Stabilization. *Cell.Physiol.Biochem.* 46:2460-2470. doi: 10.1159/000489652.

Terzibasi, E., C. Lefrançois, P. Domenici, N. Hartmann, M. Graf, and A. Cellerino. 2009. Effects of dietary restriction on mortality and age-related phenotypes in the short-lived fish Nothobranchius furzeri. *Aging Cell.* 8:88-99. doi: 10.1111/j.1474-9726.2009.00455.x.

Terzibasi, E., D.R. Valenzano, M. Benedetti, P. Roncaglia, A. Cattaneo, L. Domenici, and A. Cellerino. 2008. Large Differences in Aging Phenotype between Strains of the Short-Lived Annual Fish Nothobranchius furzeri. *PloS One.*3:e3866. doi: 10.1371/journal.pone.0003866.

Thiruvoth, F.M., D.P. Mohapatra, D. Kumar, S.R.K. Chittoria, and V. Nandhagopal. 2015. Present concepts in the physiology of adult wound healing. *Plastic and Aesthetic Research.* 2:250-256. doi: 10.4103/2347-9264.158851.

Ton, C., and C. Parng. 2005. The use of zebrafish for assessing ototoxic and otoprotective agents. *Hear.Res.* 208:79-88. doi: 10.1016/j.heares.2005.05.005.

Valdesalici, S., and A. Cellerino. 2003. Valdesalici S. and Cellerino A. 2003. Extremely short lifespan in the annual fish Nothobranchius furzeri. *Proc Biol Sci.* (Suppl.) 270: 189–191. doi:10.1098/rsbl.2003.0048.

Valenzano, D.R., E. Terzibasi, A. Cattaneo, L. Domenici, and A. Cellerino. 2006. Temperature affects longevity and age-related locomotor and cognitive decay in the short-lived fish Nothobranchius furzeri. *Aging Cell.* 5:275-278. doi: 10.1111/j.1474-9726.2006.00212.x.

Wang, L., Y. Ding, X. Guo, and Q. Zhao. 2015. Role and mechanism of vascular cell adhesion molecule-1 in the development of rheumatoid arthritis. *Exp.Ther.Med.* 10:1229-1233. doi: ETM-0-0-2635.

Wendler, S., N. Hartmann, B. Hoppe, and C. Englert. 2015. Age-dependent decline in fin regenerative capacity in the short-lived fish Nothobranchius furzeri. *Aging Cell.* 14:857-866. doi: 10.1111/acel.12367.

Werner, S., T. Krieg, and H. Smola. 2007. Keratinocyte-fibroblast interactions in wound healing. *J.Invest.Dermatol.*127:998-1008. doi: S0022-202X(15)33382-0.

Whitehead, G.G., S. Makino, C.L. Lien, and M.T. Keating. 2005. Fgf20 is Essential for Initiating Zebrafish Fin Regeneration. *Science.* 310:1957-1960. doi: 310/5756/1957.

Wilcox, J.R., M.J. Carter, and S. Covington. 2013. Frequency of debridements and time to heal: a retrospective cohort study of 312 744 wounds. *JAMA Dermatol.* 149:1050-1058. doi: 10.1001/jamadermatol.2013.4960.

Wilkinson, H.N., and M.J. Hardman. 2020. Wound healing: cellular mechanisms and pathological outcomes. *Open Biol.* 10:200223. doi: 10.1098/rsob.200223.

Witte, M.B., T. Kiyama, and A. Barbul. 2002. Nitric oxide enhances experimental wound healing in diabetes. *Br.J.Surg.* 89:1594-1601. doi: 10.1046/j.1365-2168.2002.02263.x.

Wourms, J.P. 1972. The developmental biology of annual fishes. 3. Pre-embryonic and embryonic diapause of variable duration in the eggs of annual fishes. *J.Exp.Zool.* 182:389-414. doi: 10.1002/jez.1401820310.

Wu, Y., C. Chang, A. Kao, B. Hsi, S. Lee, Y. Chen, and I. Wang. 2015. Hypoxia-induced retinal neovascularization in zebrafish embryos: a potential model of retinopathy of prematurity. *PloS One.* 10(5):e0126750. doi: 10.1371/journal.pone.0126750.

Xia, Y., Y. Zhao, J.W. Tyrone, A. Chen, and T.A. Mustoe. 2001. Differential Activation of Migration by Hypoxia in Keratinocytes Isolated from Donors of Increasing Age: Implication for Chronic Wounds in the Elderly. *J.Invest.Dermatol.*116:50-56. doi: 10.1046/j.1523-1747.2001.00209.x.

Ye, J., G. Coulouris, I. Zaretskaya, I. Cutcutache, S. Rozen, and T.L. Madden. 2012. Primer-BLAST: A tool to design target-specific primers for polymerase chain reaction. *BMC Bioinformatics.* 13:134. doi: 10.1186/1471-2105-13-134.

Žák, J., and M. Reichard. 2020. Good performance of turquoise killifish (Nothobranchius furzeri) on pelleted diet as a step towards husbandry standardization. *Scientific Reports.* 10. doi: 10.1038/s41598-020-65930-0.

Zhang, X., Y. Lan, J. Xu, F. Quan, E. Zhao, C. Deng, T. Luo, L. Xu, G. Liao, M. Yan, Y. Ping, F. Li, A. Shi, J. Bai, T. Zhao, X. Li, and Y. Xiao. 2019. CellMarker: a manually curated resource of cell markers in human and mouse. *Nucleic Acids Res.* 47:D721-D728. doi: 10.1093/nar/gky900.

Zhao, A., H. Qin, and X. Fu. 2016. What Determines the Regenerative Capacity in Animals? *Bioscience.* 66:735-746. doi: 10.1093/biosci/biw079.

Zhu, Y., Y. Wang, Y. Jia, J. Xu, and Y. Chai. 2019. Roxadustat promotes angiogenesis through HIF-1α/VEGF/VEGFR2 signaling and accelerates cutaneous wound healing in diabetic rats. *Wound Rep and Reg.* 27:324-334. doi: 10.1111/wrr.12708.

Ziche, M., L. Morbidelli, E. Masini, S. Amerini, H.J. Granger, C.A. Maggi, P. Geppetti, and F. Ledda. 1994. Nitric oxide mediates angiogenesis in vivo and endothelial cell growth and migration in vitro promoted by substance P. *J.Clin.Invest.* 94:2036-2044. doi: 10.1172/JCI117557.

# 8. Appendices

## 8.1 Appendix 1: Decapsulation of *Artemia*

Approximately 20 g of *Artemia* cysts (Ocean Nutrition) were hydrated in 16 g/l salt (Royal Nature) water in a hatching cone attached to aeriation. After this, 94 ml of precooled salt water and 7,5 ml of 40 % NaOH (Fisher Scientific) were added in the hatching cone. Finally, 300 ml of 5 % household hypochlorite was added and the color reaction in the cone was carefully followed. During the decapsulation of *Artemia,* the color of the prepared solution in cone will change from brown to orange. Following color reaction, the cysts were collected on a collection sieve and flushed with running tap water. After this, the cysts in the sieve were placed in 0.1 g/100 ml sodium thiosulfate (Fluka) for 1 minute, rinsed with tap water and finally also with 16 g/l salt water. In order to dehydrate the cysts, 1000 ml of super-saturated brine (salt content 400 g/l) was added in the cone together with the cysts. Aeriation was connected and 18-hour incubation at room temperature was started. After incubation, the cysts in brine were aliquoted to 50 ml falcon tubes and stored at 4ºC for further use. During the raising of the juvenile fish approximately 30 ml of cysts in brine were added in hatching cone daily with 1 liter of 16 g/l salt water and incubated for 18 hours at the temperature of 28°C before serving them to fish.

## 8.2 Appendix 2: Evaluation of the primers

The expression of angiogenesis-related genes *vcam1, tie1, cd34* and *vegf* were analyzed in the present study. Also, primers for lymphatic vessel endothelial hyaluronan receptor 1 *(lyve1)* and melanoma cell adhesion molecule *(mcam)* were tested, but these primers did not work. Housekeeping genes tata-box binding protein *(tbp),* insulin receptor *(insr)* and hypoxanthine guanine phosphoribosyl transferase *(hprt)* were tested for their potential as normalization genes. All of the tested primers for housekeeping genes worked, but as hypoxia may potentially downregulate the expression of *insr* (Arcidiacono et al., 2020), it was decided to select either *tbp* or *hprt.* As no differences between the expression were seen between them, *tbp* was randomly selected as the normalization gene for calculating relative quantification values. Tested primers and their sequences are listed in table 1. The selected primers for each gene were evaluated for the specificity of

the amplification signal. Primers were considered inadequate if multiple peaks as an indicator of off-target amplification were observed in melting curves. Examples for evaluating the suitability of tested primers are presented in figure 1.

**Table 1.** Primers selected and tested for their functionality in the study with their sequences and references.

| **Gene** | **Forward/reverse** | **Functionality (yes/no)** | **Reference** |
|---|---|---|---|
| *cd34* | AGATGTTGTCTGCAAGGGCA/ CCTGTAACGTCATCTTCCACG | yes | Present study |
| *hprt* | TGAGATCAGAGTGATCGGT/ GCTACTTTAACCATTTTGGGAT | yes | Hartmann et al., 2009 |
| *insr* | TGCCTCTTCAAACCCTGAGT/ AGGATGGCGATCTTATCACG | yes | Wendler et al., 2015; Hartmann et al., 2009 |
| *lyve1* | ACGGATCAACAGGAGCAAAAG/ TCTTGTCGGAGCAACGTCTT | no | Present study |
| *mcam* | AGTGAAAATCAAGAGCAAAGGTG T/ CGCCGCCCTTTATTTACTGG | no | Present study |
| *tbp* | AGCGTTTTGCTGCCGTCATA/ TTGACTGCTCCTCACTTTTGG | yes | Leggieri et al., 2019; Hartmann et al., 2009 |
| *tie1* | CGCCATCCGGAAAACATTGG/ GGACGAAATTAGCAGTGCCG | yes | Present study |
| *vcam* | ATGTTGAGGTGCTTCCCAGG/ CGGGATCTGAAGGGAAGGAAAA | yes | Present study |
| *vegfa* | AAGCCGAGAAGA TGAGAGCG/ TGTCAGACCAAGGGGAA TGC | yes | Kosonen, 2020 |

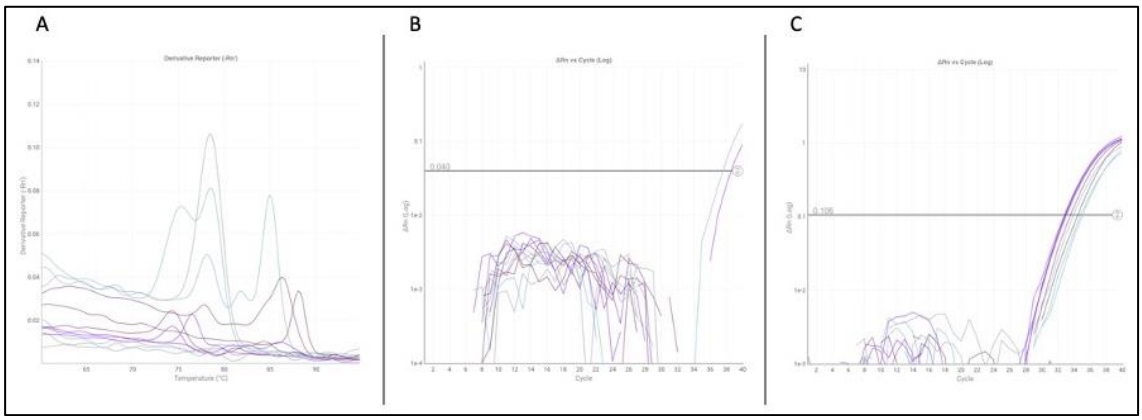


**Figure 1.** Evaluation of the tested primers was done based on amplification and melting plots. A) Primers for *mcam* showed several peaks in melting plot, which is an indicator of nonspecific amplification. B) Hardly any amplification was seen with the primers for *lyve1*. C) Primers for *tbp* showed specificity in amplification signal.

## 8.3 Appendix 3: qRT-PCR settings

qRT-PCR settings used in the present study are listed in table 1.

**Table 1.** qRT-PCR settings used in the study. Retrieved from Thermo Fisher Cloud application.

| Phase | Temperature | Time | Ramp speed | Cycles |
|---|---|---|---|---|
| Hold:<br>Step 1: UDG activation | 50ºC | 2 min. | 1.6 ºC/sec | - |
| Hold:<br>Step 2: Dual-Lock DNA polymerase activation | 95ºC | 2 min. | 1.6 ºC/sec | - |
| PCR:<br>Step1: Denaturation | 95ºC | 15 sec. | 1.6 ºC/sec | 40 |
| PCR:<br>Step 2: Annealing and extending | 60ºC | 1 min. | 1.6 ºC/sec | 40 |
| Melt Curve:<br>Step 1: Denaturation | 95ºC | 15 sec. | 1.6 ºC/sec | - |
| Melt Curve:<br>Step 2: Annealing | 60ºC | 1 min. | 1.6 ºC/sec | - |
| Melt Curve:<br>Step 3: Denaturation (dissociation) | 95ºC | 15 sec. | 0.05 ºC/sec. | - |